EARLY CAMBRIAN HUMID, TROPICAL, COASTAL PALEOSOLS FROM MONTANA, USA

GREGORY J. RETALLACK
Department of Geological Sciences, University of Oregon, Eugene, Oregon 97403, USA
e-mail: gregr@uoregon.edu

Abstract: A putative Precambrian paleosol mapped at the unconformity between the Cambrian Flathead Sandstone and Belt Supergroup at Fishtrap Lake, Montana, was found instead to be a succession of paleosols forming the basal portion of the Flathead Sandstone. Early Cambrian age of these paleosols comes from stratigraphic ranges of associated marine trace fossils: *Bergaueria hemispherica*, *Didymaulichnus lyelli*, *Torrowangea* sp. indet., and *Manykodes pedum*. Instead of a single strongly developed paleosol on top of the Belt Supergroup with a smooth geochemical depth function, five successive geochemical and petrographic spikes were interpreted as so many individual paleosols within a short sedimentary sequence of red beds, overlying brecciated and little-weathered Belt Supergroup. The most weathered intervals (paleosol A horizons) are purple–red in color (Munsell weak red, 7.5R 4/2) and massive to hackly, whereas intervening marine siltstones are planar bedded and purple–gray (Munsell dark reddish gray, 7.5R 4/1). The massive to hackly appearance comes from blocky to platy peds defined by argillans and is also the result of pervasive bioturbation of two distinct kinds: drab-haloed filament traces and ferruginized-organic filaments. In thin section, the filaments are circular as well as elliptical and elongate and of presumed microbial origin. The filament-rich (A) horizons are also defined by magnetic susceptibility and show petrographic evidence of significant weathering (depleted abundance of rock fragments, feldspar, and mica compared with lower horizons). Additional evidence of weathering comes from chemical analyses showing net loss of mass and weatherable elements within a profile. These lines of evidence indicate that Montana estuarine landscapes during the earliest Cambrian were colonized by filamentous organisms in a tropical humid paleoclimate, rather than the frigid conditions documented elsewhere during the Late Ediacaran and Early Cambrian.

Key words: Cambrian, Montana, paleosol, trace fossil, paleoclimate

INTRODUCTION

Precambrian paleosols are mainly known from major geological unconformities (Rye and Holland 1998), whereas Phanerozoic paleosols are mainly known from sedimentary sequences (Retallack 2009a, 2009b, 2009c). Is this difference real, or does it reflect the difficulty of identifying in Precambrian sediments successive paleosols that lack fossil root traces and other obvious indications common in post-Silurian paleosols (Driese et al. 1997, Driese and Mora 2001, Retallack and Huang 2011)? This article advances criteria for recognition of Early Paleozoic and Precambrian paleosols in sedimentary sequences so that paleopedology can expand beyond major geological unconformities. Many Phanerozoic unconformity paleosols preserve superposed weathering signals and groundwater alteration that are difficult to unravel (Ollier and Pain 1996, Taylor and Eggleton 2001). In Phanerozoic sequences, paleosols of short duration of formation and simple profile form, repeated as populations of similar profiles within paleosol successions, have been the easiest to interpret because they are comparable in time and mode of formation to Holocene soils (Retallack 2001). In contrast, in Precambrian rocks it has been easy to find unconformities and their unusually thick and deeply weathered paleosols (Rye and Holland 1998), but interpretations have proven controversial (Ohmoto 1996).

This article develops criteria for recognition and interpretation of pre-Silurian paleosols (Driese et al. 1995; Retallack 2012a, 2012b), with a detailed account of earliest Cambrian paleosols in Montana. Few Cambrian paleosols have been recognized or studied in detail (Ávaro et al. 2003; Retallack 2008, 2009a, 2011b), despite abundant and widespread Cambrian nonmarine rocks (Daily et al. 1980; Moore 1990; Went 2005; Rose 2006; Davies and Gibling 2010; Davies et al. 2011; Hagadorn et al. 2011a, 2011b). Paleosols studied here were reported as a Precambrian paleosol profile on the unconformity between the Belt Supergroup and Flathead Sandstone (Harrison et al. 1986), but detailed petrographic and geochemical analysis now reveals that this is a sedimentary sequence of red beds with several paleosols between an erosional surface of the Belt Supergroup and sandy marine facies of the Flathead Sandstone. The Early Cambrian, rather than Proterozoic, age of these red beds comes from a newly discovered assemblage of trace fossils.

MATERIALS AND METHODS

The study area is immediately east of Fishtrap Lake, which is accessible via forest road numbers 5, 56, 516, and 7953, 32 miles north of Thompsons Falls, Sanders County, western Montana (Fig. 1). Red beds (Fig. 2A, B) with trace fossils (Fig. 3) are exposed along a disused road immediately west of the bridge over the Radio Creek outlet of Fishtrap Lake (N47.86200°, W115.19706°). Trace fossil specimens F113699 to 113724 and F115957 to 15982 are archived in the Condon Fossil Collection, Museum of Natural and Cultural History at the University of Oregon in Eugene, Oregon.

The red beds were sampled for preparation of petrographic thin sections, which were point-counted (500 points) to determine grain size and mineral composition using a Swift automated counter and stage (Figs. 4, 5; Table 1). Samples were analyzed for magnetic susceptibility using an SI-2 meter by R.D. Elmore at the University of Oklahoma (Norman), as described elsewhere (Retallack et al. 2003). Samples of the Cool pedotype were collected for laboratory analyses (Table 2), as follows: major and trace element geochemical analysis by XRF and analysis of ferrous iron by potassium dichromate titration (by ALS Chemex of Vancouver, British Columbia, Canada, using CANMET SDST standard-2 of British Columbia granodiorite). Molar ratios were also calculated from bulk chemical analyses to give products over reactants of common soil-forming chemical processes (Retallack 2001). A more detailed accounting of geochemical change following the method of Brimhall et al. (1992) is mass transfer of elements in a soil at a given horizon ($\tau_{w,j}$ in moles), calculated from the bulk density of the soil (ρ_w in g/cm^3) and parent material (ρ_p in g/cm^3)

New Frontiers in Paleopedology and Terrestrial Paleoclimatology | DOI: 10.2110/sepmsp.104.09
SEPM Special Publication No. 104, Copyright © 2013
SEPM (Society for Sedimentary Geology), ISBN 978-1-56576-322-7, p. 257–272.

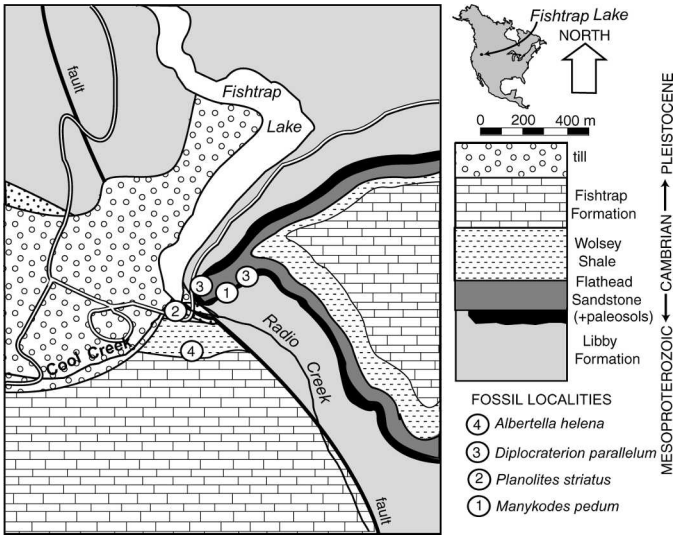

FIG. 1.—Geological map and Cambrian fossil localities near Fishtrap Lake, Sanders County, Montana. All units except Pleistocene till and paleosols in the lower Flathead Sandstone are marine.

and from the chemical concentration of the element in soils ($C_{j,w}$ in weight %) and parent material ($C_{p,w}$ in weight %). Changes in the volume of soil during weathering are called "strain" by Brimhall et al. (1992) and are estimated from an immobile element in soil (such as Ti, used here) compared with parent material ($\varepsilon_{i,w}$ as a fraction). The relevant Eqs. 1 and 2 (below) provide the basis for calculating divergence from parent material composition due to soil formation:

$$\tau_{j,w} = \left[\frac{\rho_w \times C_{j,w}}{\rho_p \times C_{j,p}}\right][\varepsilon_{i,w} + 1] - 1; \quad (1)$$

$$\varepsilon_{i,w} = \left[\frac{\rho_p \times C_{j,p}}{\rho_w \times C_{j,w}}\right] - 1. \quad (2)$$

These calculations were performed for one of the Cambrian paleosols and also for Miocene paleosols from Pakistan. These Miocene paleosols were buried by 2 km of overburden and have undergone common early diagenetic alterations such as burial gleization, decomposition, and ferric hydroxide dehydration (Retallack 1991), so they offer a clearer comparison with Cambrian paleosols with similar burial history, compared to modern soils. This is an isotaphonomic approach to paleopedology.

GEOLOGICAL AGE

Newly discovered marine trace fossils (Fig. 3) now indicate that red beds of Radio Creek are of the earliest Cambrian (542 Ma; Gradstein et al. 2004), lowest Fortunian Stage (Landing et al. 2007). This determination provides additional support for Rb-Sr ages of 555 ± 18 Ma for shales and of 542 Ma for a single authigenic glauconite of the Flathead Sandstone in Montana (Chaudhuri and Brookins 1969). These red beds have been regarded as a single paleosol at the disconformity between the Neoproterozoic Libby Formation of the uppermost Belt Supergroup and the Cambrian Flathead Sandstone (Harrison et al. 1986), as an outlier of the Pilcher Formation within the uppermost Belt Supergroup (Winston et al. 1977), or as an outlier of the Windermere Supergroup (Retallack et al. 2003). These micaceous, quartz-poor red beds contrast with red orthoquartzites of the Pilcher Formation (Nelson and Dobell 1961), which have, in addition, indications of a glacial climate (Illich et al. 1972) incompatible with geochemical differentiation of the paleosols studied here (Figs. 4, 5). The Windermere Supergroup of western Canada is Neoproterozoic to Early Cambrian (736–540 Ma; Colpron et al. 2002) and has metamorphosed equivalents in Idaho (Lund et al. 2003). The Mesoproterozoic Belt Supergroup has been radiometrically dated at 1401 to 1454 Ma (Evans et al. 2000).

Newly Discovered Trace Fossils

The geological age of the red beds of Radio Creek is best constrained by a newly discovered suite of trace fossils: *Manykodes pedum* (Fig. 3D), *Bergaueria hemispherica* (Fig. 3E), *Didymaulichnus lyelli* (Fig. 3B), and *Torrowangea* sp. indet. (Fig. 3C).

The most age-diagnostic of these trace fossils is *Manykodes pedum* (Seilacher) Dzik (2005), which has been used to define the earliest Cambrian (Landing et al. 2007) but also has been found 4.4 m below the Global Stratigraphic Stratotype (GSSP) for the base of the Cambrian in the stratotype section at Fortune Head, Newfoundland (Gehling et al. 2001). Until recently, this ichnospecies has been assigned to *Phycodes* (Häntzschel 1975), *Trichophycus* (Geyer and Uchman 1995), and *Treptichnus* (Jensen 1997). *Manykodes pedum* is a burrow that has alternate branches outward and upward and is preserved as a filled tube (exichnion of Martinsson [1970]). Specimens from Fishtrap Lake have tubes measuring 3.4 to 3.9 mm wide, which turn to branch at intervals of 6.6 to 8.7 mm, which is a shorter interval than has been identified for the other known ichnospecies, *Manykodes rectangulare* (Dzik 2005).

Other trace fossils of the red beds of Radio Creek are Early Cambrian and are not known to range down into the latest Precambrian (Jensen et al. 1998, 2006, 2007; Grazhdankin and Krayushkin 2007). A single specimen of *Bergaueria hemispherica* Crimes et al. (1977) from Fishtrap Lake lacks either strong (as in *Bergaueria radiata*) or faint radial ribs (as in *Bergaueria perata*) or thick walls (as in *Bergaueria langi*). With an elliptical neck measuring 24 to 20 mm in diameter and with a basal portion measuring 26 to 22 mm in diameter, the specimen from Fishtrap Lake is only half the size of type specimens of *Bergaueria hemispherica* from the Cayetano Beds of the Cándana Quartzite of Spain (Crimes et al. 1977, Pemberton et al. 1988, Pemberton and Magwood 1990). *Bergaueria hemispherica* is best known from the Early Cambrian (Crimes et al. 1977) and may range through to the Cretaceous (Leszczyński 2004).

Specimens of *Didymaulichnus lyelli* (Rouault) Young (1972) are hypichnial ridges (of Martinsson [1970]), 9.6 to 9.5 mm wide, with shallow central grooves that are 1.2 to 1.9 mm wide. Trails with more sharply defined lateral margins include *Archaeonassa* (Yochelson and Fedonkin 1997) and *Aulichnites* (Fedonkin 1985). Trails with much deeper central seams include *Mattaia miettensis*, *Mattaia tirasensis,* and *Mattaia meanderiformis* (Dzik 2005). The Fishtrap Lake trails do not form irregular circles like *Taphrelminthopsis circularis* (Crimes et al. 1977, Jensen et al. 1998) or networks like *Olenichnus irregularis* (Fedonkin 1985). Specimens from Fishtrap Lake also lack the joint-like features of *Didymaulichnus roualti* (Häntzschel 1975), and undulation of *Didymaulichnus alternatus* (Jensen and Mens 2001). *Didymaulichnus lyelli* ranges from Late Ediacaran to Triassic and perhaps Miocene (Kumpulainen et al. 2006) or Quaternary (Ekdale and Lewis 1991).

Torrowangea rosei Webby (1970) is a narrow, beaded, hypichnial ridge. The burrows from Fishtrap Lake are similar in form, but include exichnia (of Martinsson [1970]) that are filled with silt coarser than clayey silt matrix and are slightly larger (maximum width of 4.6–5.1 mm; width at constriction of 3.4–3.6 mm), and so are identified here as *Torrowangea* sp. indet. Another peculiarity of the Fishtrap Lake specimens is that isolated segments (Fig. 3C, lower right) pass upward

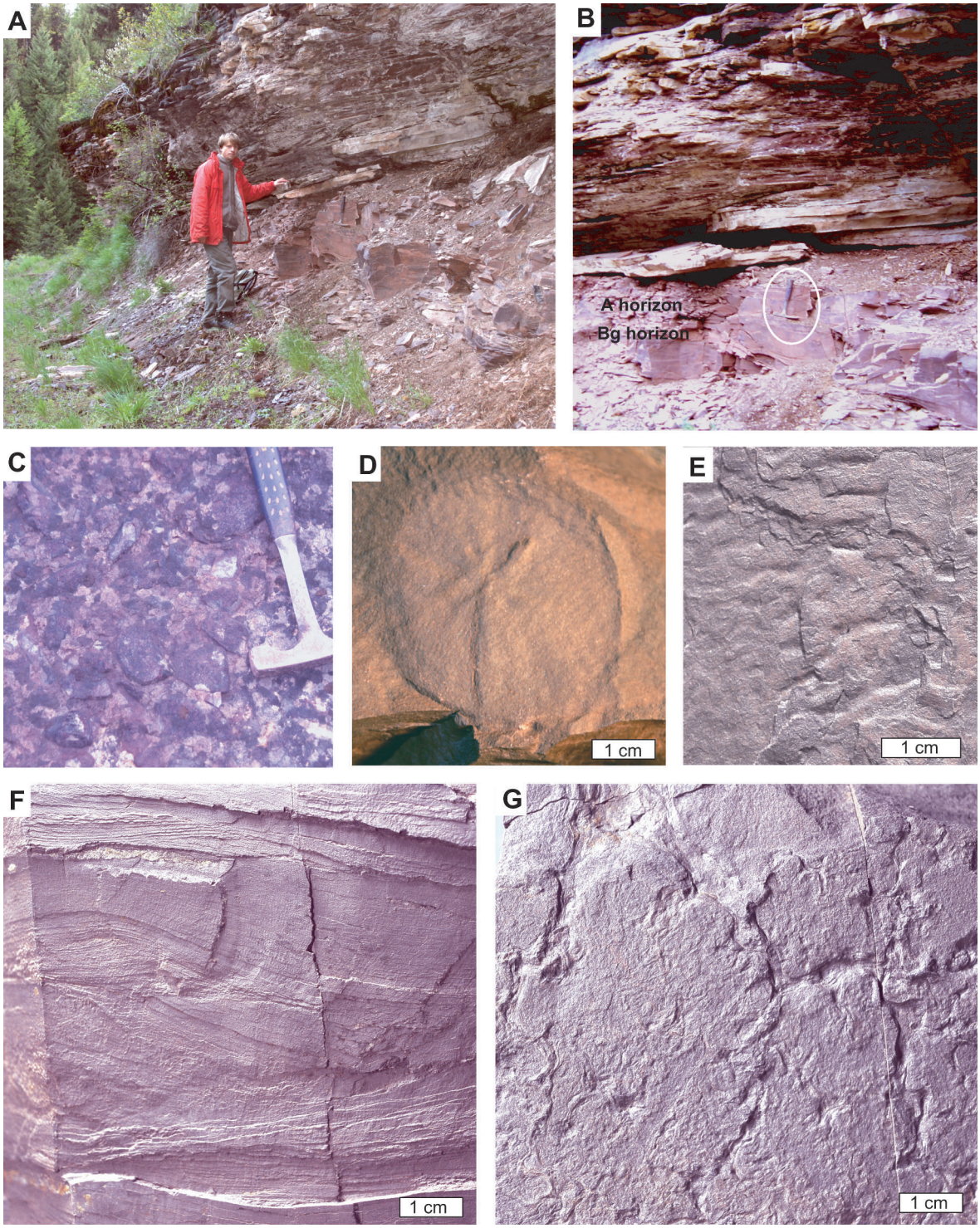

FIG. 2.—Outcrop **A**); Radio paleosol **B**); conglomerate of Flathead Sandstone **C**); cast of pyrite sun **D**); *Kinneyia* wrinkle marks **E**); opposed ripple marks, mud flasers, and scour-and-fill **F**); and oscillation desiccation polygons **G**) from Fishtrap Lake, Montana. Scales provided by Dima Grazhdankin (A) and hammers (B, C). Specimen numbers (Condon Collection, University of Oregon) and stratigraphic levels (cm in Fig. 4) are F113703B at −40 cm (D), F113700 at −15 cm, R4159 at −30 cm (E), and F115976 at −35 cm (G).

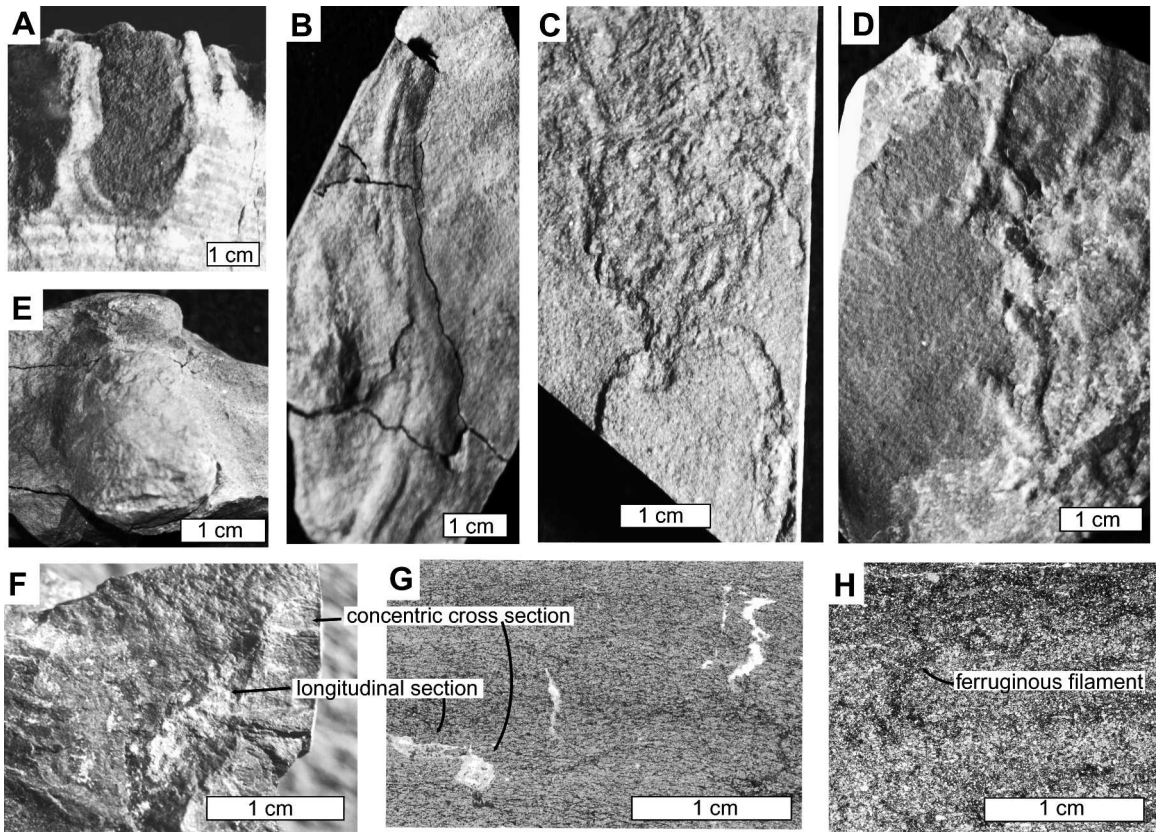

FIG. 3.—Trace fossils, including *Diplocraterion parallelum* **A**), *Didymaulichnus lyelli* **B**), *Torrowangea* sp. indet. **C**), *Manykodes pedum* **D**), *Bergaueria hemispherica* **E**), *Prasinema gracile* **F, G**), and strata-transgressive ferruginous filamentous structures **H**). Specimen numbers (Condon Collection, University of Oregon) and stratigraphic levels (cm in Fig. 4) include F115964 at +50 cm (A), F115970 at −60 cm (B), F115961B at −60 cm (C), F115760A at −60 cm (D), F115963 at −20 cm (E), F113698 at −5 cm (F), R3581 at −10 cm (G), and R3585 at −35 cm (H).

into a confused tangle of similar segments (Fig. 3C, upper). Simple constrictions distinguish *Torrowangea* from en echelon burrows such as *Streptichnus narbonnei* (Jensen and Runnegar 2005). The stratigraphic range of *Torrowangea* is latest Ediacaran to Ordovician (Vintaned et al. 2006, Retallack 2009a).

Other Cambrian Fossils

The red beds at Fishtrap Lake also include subvertical clayey tubules with a green–gray halo, identical to *Prasinema gracile* (Retallack 2011b). These can be seen to have a central clayey fill that is dark gray in color (Fig. 3F, G) and a flanking halo of gray–green color (Munsell greenish gray, 5G 5/1), which is about equal in width to the central tube. Viewed in longitudinal section these are subparallel tubes bending and branching through the red matrix, but in cross section the inner tube and outer halo appear concentric (Fig. 3F, G). This occurrence is only a slight range extension for *Prasinema*, which has already been recorded from Early Cambrian paleosols associated with *Diplocraterion* in the Parachilna Formation of South Australia (Retallack 2011b).

Quartz sandstones of the upper Flathead Sandstone near Fishtrap Lake also yielded the Early Cambrian trace fossil *Diplocraterion parallelum* Torell (1870; Fig. 3A) at two localities (N47.86229°, W115.19649° and N47.86183°, W115.19833°) and *Planolites striatus* Hall (1852) at another locality near the top of the quartzites (Fig. 1; N47.86193°, W115.20044°). *Cruziana* has been reported from the upper Flathead Formation elsewhere in this region (Aadland 1985), indicating an age no older than the first appearance of trilobites (ca. 524 Ma; Gradstein et al. 2004).

In an old roadcut located 2 km southwest of Fishtrap Lake (N47.86068°, W115.19963°) the overlying lower Wolsey Shale yields abundant articulated trilobites (*Albertella helena, Kochina gordonensis, Strotocephalus gordonensis, Ptarmigania gordonensis,* and *Vanuxemella contracta*), as well as brachiopods (*Acrothele colleni* and *Micromitra scuptilis*) and hyoliths (*Hyolithus convexus*). The same assemblage has been recorded from the Wolsey and Gordon shales elsewhere in Montana (Walcott 1917, Keim and Rector 1964, Bush 1989), in the *Albertella* zone of early Middle Cambrian age (ca. 508 Ma; Gradstein et al. 2004).

SEDIMENTOLOGY

Cliffs of underlying Libby Formation of the Belt Supergroup rim the road around Fishtrap Lake to the north and west and are disconformably overlain by a breccia of redeposited Libby Formation and then by red beds and sandstone. These three facies are all included

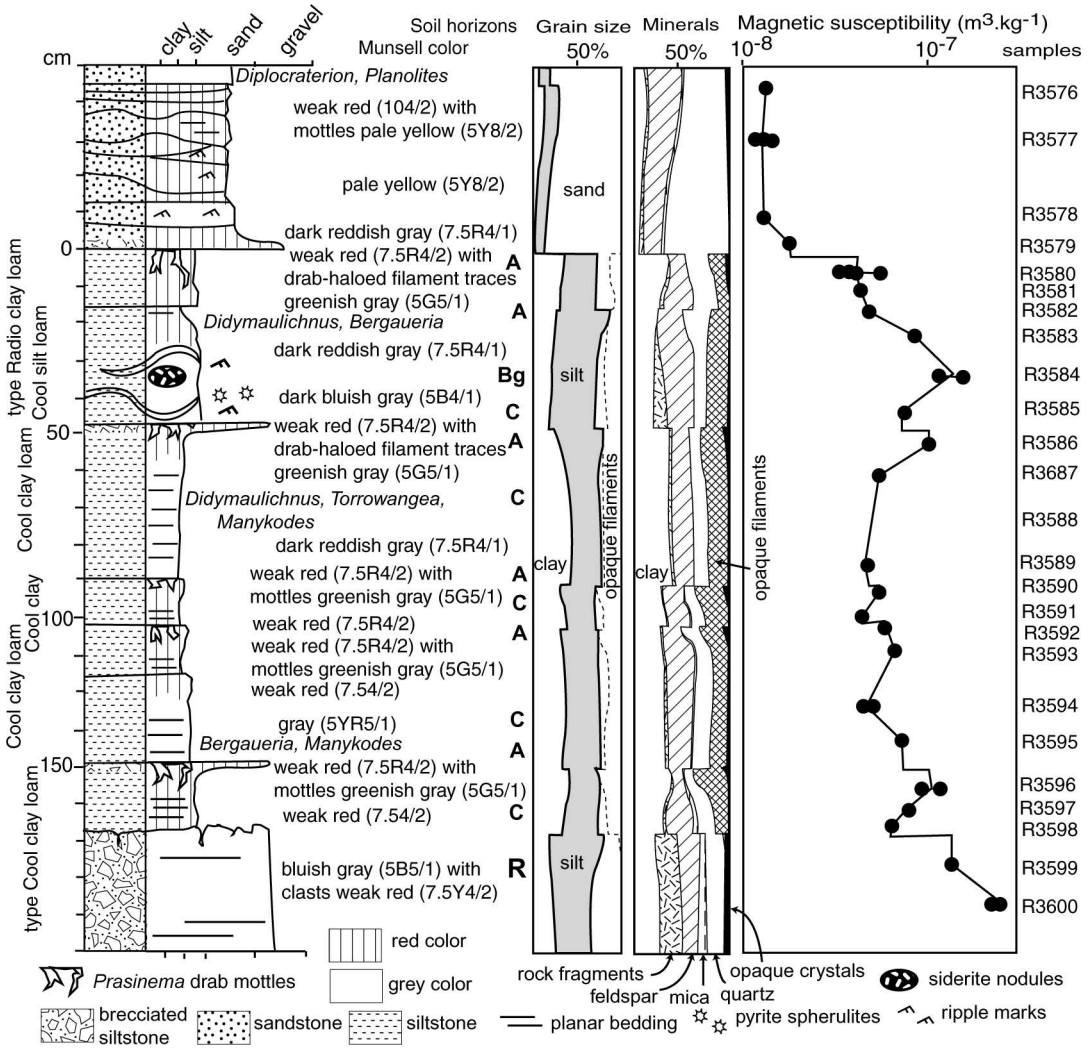

FIG. 4.—Measured section of red beds of lower Flathead Sandstone near Fishtrap Lake, Sanders County, Montana. Grain size and mineral composition are from point counting of petrographic thin sections. Magnetic susceptibility data are from Retallack et al. (2003).

here within the basal Flathead Sandstone, which is overlain by Wolsey Shale and then Fishtrap Formation to the south and east (Harrison et al. 1986, Bush 1989).

Sedimentary Facies

Gray breccia disconformably overlies intact Libby Formation, although the contact is difficult to see because the clasts of the breccia are identical in color and lithology to Libby Formation, which is a green–gray, heterolithic siltstone and shale, with common ripple marks and mud cracks (Harrison et al. 1986). The lower contact of gray breccia with undisturbed Libby Formation is poorly exposed but is gray, with no discoloration due to ferruginization or other chemical weathering.

The red bed facies consists of heterolithic purple–red (Munsell weak red, 7.5R 4/2) siltstones and purple–gray (Munsell dark reddish gray, 7.5R 4/1) shaley siltstones (Fig. 2A, B). Sedimentary structures observed in the silty beds include scour-and-fill, ripple marks, clay drapes (Fig. 2F), wrinkle marks (Fig. 2E), and planar lamination. One bed of siltstone and shale includes several ripple trains with opposing paleocurrent directions (Fig. 2F). One horizon has large (3–4 cm in diameter) claystone casts (Fig. 2D) of what appear to have been pyrite spherulites (Bannister 1932, Cloud 1973). Another horizon has ellipsoidal to lobate dark gray siderite nodules (Fig. 4).

Sandstone facies overlie red beds with a distinctive basal lag of subangular pebbles with thick rinds of purple–red iron manganese, set within a groundmass of strongly ferruginized sandstone (Fig. 2C). Pebbles are not found in the overlying sandstone, which is coarse to medium grained with planar cross-bedding, parting lamination, and flaggy bedding some 2 to 5 cm thick (Fig. 2B).

Sedimentary Paleoenvironments

Flathead Sandstone has been interpreted as a former barrier bar and shoreface (Aadland 1985), and such a paleoenvironment is compatible with features observed near Fishtrap Lake, including the marine trace fossil *Diplocraterion* (Fig. 3A). A basal shale breccia to the sandstone has flat surfaces similar to ventifacts but lacks regularity of form and direction found in true ventifacts (Schlyter 2006), nor does this breccia show the edgewise fabric or exotic clasts characteristic of storm or

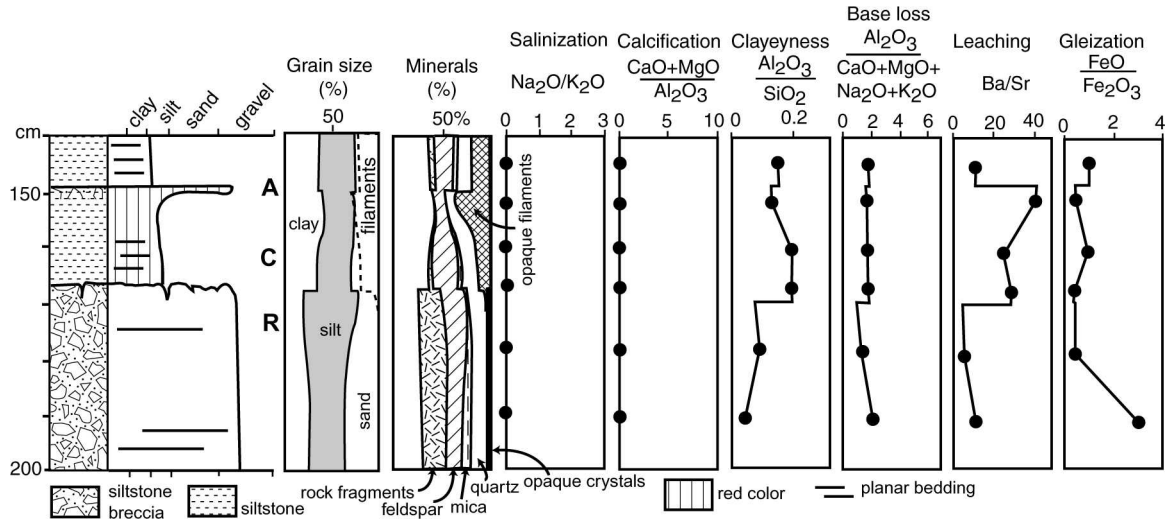

FIG. 5.—Petrographic composition and molecular weathering ratios from whole-rock major-element composition determined by XRF (Tables 1, 2) of the Cool clay loam paleosol (−150 cm in Fig. 4) at Fishtrap Lake, Montana.

tsunami beds (Pratt 2002). This breccia was not noticed until it was excavated because it is the same color and texture as the unbrecciated Libby Formation below, with a few wisps of red siltstone that have fallen down between cracks. These are unweathered clasts of Libby Formation and not corestones of a weathering profile, like those known from Precambrian paleosols at major geological unconformities (Retallack and Mindszenty 1994). This thin shale breccia is interpreted here as a shoreline talus, like those widespread in fluvial and intertidal

TABLE 1.—Petrographic data (volume percent) on red beds of Flathead Sandstone.*

Spec.	Sand	Silt	Clay size	Quartz	Feldspar	Clay mineral	Opaque	Filament	Mica	Rock fragments	Description	Interpretation
3576	79.0	12.6	8.4	55.2	29.4	10.4	1.4	0	1.6	2.2	silasepic granular	barrier bar sand
3577	70.0	18.0	12.0	52.6	28.8	11.8	2.2	0	0.8	3.8	silasepic granular	barrier bar sand
3578	72.0	19.4	8.6	58.8	28.6	7.6	2.4	0	0	2.6	silasepic granular	barrier bar sand
3579	83.0	9.6	7.4	65.8	19.6	5.6	1.8	0	0.6	6.6	silasepic intertextic	barrier bar sand
3580	29.2	37.0	33.8	17.4	17.8	36.8	2.8	21.8	3.4	0	mosepic porphyroskelic	Radio clay loam A
3581	32.4	40.2	27.2	22.2	29.2	0.4	0.4	14.8	1.8	4.0	insepic porphyroskelic	Radio clay loam A
3582	15.2	58.8	26.0	18.0	28.2	28.6	2.2	15.4	3.6	4.0	insepic porphyroskelic	Radio clay loam A
3583	31.2	45.8	23.0	21.8	34.8	21.6	0.6	15.6	4.2	1.4	mosepic porphyroskelic	Radio clay loam Bg
3584	29.8	47.4	22.8	21.2	30.6	21.4	2.2	18.4	2.6	3.6	insepic porphyroskelic	Radio clay loam Bg
3585	36.8	42.8	20.4	13.6	21.0	21.0	1.8	22.4	4.6	15.6	argillasepic intertextic	Radio clay loam C
3586	26.4	38.8	34.8	10.6	18.4	37.2	0.4	29.8	1.4	2.2	bimasepic porphyroskelic	Cool silt loam A
3587	29.0	41.2	29.8	9.6	19.6	34.2	0.4	29.4	3.6	3.2	insepic intertextic	Cool silt loam C
3588	22.0	39.4	38.6	12.4	19.0	40.4	3.6	19.4	2.2	2.8	insepic agglomeroplasmic	lagoonal shale
3589	24.0	34.6	41.4	8.0	16.2	43.8	0.6	28.8	1.6	1.0	insepic porphyroskelic	lagoonal shale
3590	28.6	41.6	29.8	13.4	19.0	30.6	0.6	33.4	2.4	0.6	mosepic porphyroskelic	Cool clay A
3591	29.0	37.0	34.0	16.0	24.4	35.2	1.0	34.0	2.2	0	insepic porphyroskelic	Cool clay C
3592	27.8	37.2	35.0	14.4	20.4	34.0	0.6	28.0	1.8	0.8	mosepic porphyroskelic	Cool clay loam A
3593	27.8	37.0	35.2	19.4	23.8	37.6	2.2	15.6	1.0	0.4	insepic porphyroskelic	Cool clay loam C
3594	26.2	41.8	32.0	16.8	22.6	35.6	2.0	18.0	3.6	1.4	mosepic porphyroskelic	Cool clay loam C
3595	26.2	41.4	32.4	16.4	21.0	33.4	1.4	21.6	1.4	4.6	insepic porphryoskelic	lagoonal shale
3596	25.0	42.0	33.0	7.6	15.8	33.0	0.4	38.0	2.2	3.0	mosepic porphyroskelic	Cool clay loam A
3597	26.4	33.8	39.8	13.6	18.8	41.4	1.6	20.0	3.2	1.4	insepic porphyroskelic	Cool clay loam A
3598	27.8	40.6	31.6	21.8	26.0	33.6	0.8	12.6	3.6	1.6	insepic porphryoskelic	Cool clay loam C
3599	24.2	57.8	18.0	17.4	27.6	21.4	5.0	1.2	7.8	20.8	argillasepic porphyroskelic	littoral talus
3600	36.2	35.4	28.4	16.6	21.6	30.4	4.4	0	4.6	22.4	argillasepic porphyroskelic	littoral talus

* Opaque includes equant minerals such as ilmenite; elongate opaque materials are counted as organic-iron filaments. Error of these 500 point counts is ±2% for components >5%.

TABLE 2.—Chemical composition (weight percent for oxides and LOI, ppm for elements, and g/cm^3) of Cool pedotype.*

Spec.	SiO_2	TiO_2	Al_20_3	FeO	Fe_2O_3	MnO	CaO	MgO	Na_2O	K_2O	P_20_5	Ba	Sr	Y	Nb	Zr	Rb	LOI	Total	Bulk density
3593	66.42	0.53	17.14	3.99	1.16	0.02	1.37	0.14	0.17	5.24	0.03	517	30	60	15	334	218	3.82	100.29	2.71
3596	68.68	0.53	15.88	3.40	1.03	0.02	1.27	0.11	0.15	4.84	0.03	528	8	52	21	273	213	3.45	99.01	2.71
3597	60.74	0.75	20.81	3.32	1.29	0.02	1.34	0.1	0.09	6.76	0.03	771	18	71	22	284	284	4.23	99.77	2.67
3598	61.53	0.76	20.71	3.23	1.03	0.06	1.40	0.14	0.13	6.54	0.03	761	16	70	21	272	272	4.28	100.12	2.71
3599	67.74	0.29	11.03	9.29	2.51	0.03	1.51	0.12	0.09	2.50	0.04	294	34	28	8	98	98	3.66	99.41	2.73
3600	82.76	0.23	7.10	1.70	2.32	0.02	0.67	0.1	0.05	1.36	0.02	183	10	26	16	81	81	2.22	98.92	2.68
Error	2.705	0.06	0.83		0.0395	0.025	0.22	0.18	0.11	0.13	0.035							0.35		0.02

* Oxides, loss on ignition (LOI), and totals are in weight %; trace elements in ppm; and bulk density in g/cm^3. Analyses are by XRF with Pratt titration for FeO. Chemical errors are from 10 replicate analyses of the standard, CANMET SDMS2 (British Columbia granodioritic sand), and bulk density errors are from 10 replicates of siltstone from the Ediacara Member of the Rawnsley Quartzite, South Australia.

rock platforms flanked by cliffs (Stone et al. 1996, Aarseth and Fossen 2004, Frankel et al. 2007, Retallack and Roering 2012). Toward the south of the main fossil locality 1 (Figs. 1, 2A) the red beds and breccia thicken to 6 m, but across the fault picked out by Radio Creek unbrecciated Libby Formation is directly overlain by red sandstone. Thus, the flanking bedrock cliffs of Libby Formation had initial relief of at least 6 m.

The red beds include ripple-marked, linsel, and planar-bedded micaceous siltstones and shales, comparable with intertidal to supratidal, rather than lacustrine or fluvial, facies (Reineck and Singh 1980). Evidence for intertidal deposition comes in particular from bidirectional ripple marks (Fig. 2F), which are well known from flumes programmed for bidirectional flow (Southard et al. 1990), from modern tidal flats such as the German North Sea coast (Newton 1968) and coastal Bengal (Mukherji et al. 1994) and from ancient tidalites (Klein 1970, Greb and Archer 1995). Bidirectional ripples are common on the surface of modern tidal flats, but they are seldom preserved because of reactivation during the stronger of either ebb or flood tides (Klein 1970). Bidirectional ripples are more common on point bars of tidal estuaries than on tidal flats open to the sea, perhaps because of ebb and flood erosive-flow separation in sinuous estuaries (Mukherji et al. 1994).

Evidence of brief and repeated ancient exposure comes from desiccation cracks (Fig 2G), comparable with supratidal polygonal oscillation cracks, which form in intertidal regimes of wetting and drying (Noffke 2010). Oscillatory marginal bands derive from opening and closing, and the shallowness of these cracks, as compared with that of ordinary mud cracks and flakes (Weinberger 2001), is due to persistent deep waterlogging and algal stabilization. Fills of clay, rather than sand, and a v-shaped cross section distinguish these from syneresis cracks (Pratt 1998a). These are neither common nor deeply penetrative structures, such as molar tooth structures (Pratt 1998b), earthquake fragmented beds (Pratt 2002), or diastasis cracks (Cowan and James 1992).

The red beds also include a distinctive kind of wrinkle structure—comparable to ripple marks with wavelengths of only a few millimeters (Fig. 2E). Such *Kinneyia* microbial trace fossils are common in shallow subtidal and intertidal facies (Mata and Bottjer 2009) and have been regarded as cyanobacterial surface features (Hagadorn and Bottjer 1997), but they may also be created by shallow microbial mat deformation (Porada et al. 2008).

Marine influence is indicated by the trace fossil assemblage (Fig. 3B–E), which is within laminated parent siltstones to the paleosols (Fig. 4). However, one marine-influenced paleosol contained the presumed marine trace fossil *Bergaueria* (Fig. 3E) and a deeper horizon of pyrite spherulites (Fig. 2D), like those known from Holocene mangrove soils (Bush et al. 2004). The trace fossil assemblage of sandstones above the red beds comprise *Skolithos* ichnofacies, widely interpreted as an assemblage of beaches and barrier bars (Buatois and Mángano 2011). The trace fossil assemblage of the gray siltstones, including *Manykodes pedum,* is not assignable to an ichnofacies, because it represents an assemblage of the earliest known burrowing metazoans (Droser et al. 2002, Landing et al. 2007), predating trilobites and their otherwise-similar shallow burrowing assemblage of shallow to deep marine shales (*Cruziana* ichnofacies of Seilacher [2007]). The earliest Cambrian *Manykodes* assemblage in Newfoundland (Landing et al. 1988) and South Africa (Buatois and Mángano 2011) is considered intertidal. At Fortune Head, Newfoundland, intertidal heterolithic facies with *Manykodes* directly overlies red beds with red Entisol and Inceptisol paleosols (Landing et al. 1988; GJ Retallack, unpublished data, 2011), and the distance between *Manykodes* and paleosols in less than a meter (Gehling et al. 2001). *Cochlichnus* and *Plangtichnus* in Pennsylvanian estuarine tidalites from Kentucky (Greb and Archer 1995) form a limited assemblage of shallow burrowing trace fossils comparable with the *Manykodes pedum* assemblage.

Drab-haloed filament traces (*Prasinema gracile*) formed from burial gleization of carbonaceous filaments in paleosols and are known from both estuarine and fluvial paleosols (Retallack 2011b). These trace fossils and shaley depositional facies are comparable to Cambrian near-marine siliciclastic facies in the Billys Creek, Moodlatana and Balcoracana formations of the Flinders Ranges of South Australia (Retallack 2008). In contrast, alluvial facies of Cambrian and Ordovician age are sandy with prominent cross-bedding (Went 2005; Rose 2006; Retallack 2009a, 2009b; Davies and Gibling 2010; Davies et al. 2011).

Comparable modern clayey and silty sediments on bedrock are found in estuarine sloughs near Coos Bay, Oregon (Wilson et al. 2007). Bedrock in this part of Oregon comprises Eocene to Miocene marine sandstones, which form coastal cliffs and pocket beaches with locally derived littoral talus (Armentrout 1981, Retallack and Roering 2012). A large barrier bar sand spit separates the Coos River from the open Pacific Ocean (Lund 1973). Tidal flats behind this barrier are brown clays and silts with a variety of burrowing estuarine clams, shrimp, and worms (Oglesby 1973, McCauley et al. 1977), and supratidal flats support peaty and sulfidic salt marshes of *Salicornia virginiana* and *Distichlis spicata* (Nelson et al. 1996). This variety of marine invertebrates and vascular land plants signifies a clear difference between the modern ecosystem and the earliest Cambrian ecosystems of the *Manykodes pedum* zone, which predates both trilobites (*Cruziana*) and deep burrowing worms (*Diplocraterion*; Buatois and Mángano 2011).

The thin sequence of breccia, heterolithic red beds, and sandstone of the Flathead Sandstone at Fishtrap Lake is thus interpreted to represent,

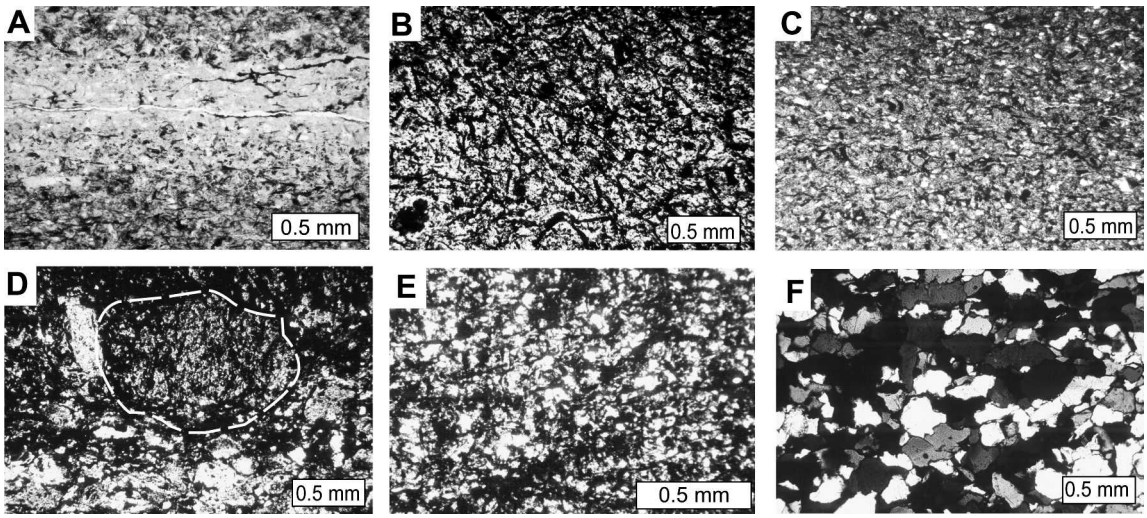

FIG. 6.—Petrographic thin sections under crossed nicols of paleosols (A, B, E) and sediments (C, D, F) of red beds (A–E) and sandstone (F), all cut vertical to bedding, from near Fishtrap Lake, Montana. Filamentous microfabrics of paleosol surfaces (A, B) are unlike laminated microfabrics of sediments (C) and are found within redeposited clasts (outlined in D). Bedding (horizontal) is disrupted by illuviation argillans (E; oblique). Flathead Sandstone is quartz-rich and layered (F). Specimen numbers (Condon Collection, University of Oregon) and stratigraphic levels (Fig. 3) are F113720 at −110 cm (A), R3586 at −50 cm (B), R3597 at −150 cm (C), R3599 at −170 cm (D), R3596 at −150 cm (E), and R3576 at +45 cm (F).

successively, littoral talus, followed by marine-influenced lagoons or estuaries, and then sandy barrier bars, confirming the regional interpretation of marine transgression noted for these rocks by Aadland (1985). Transgression continued with the offshore shale deposition of trilobite-bearing gray shales of the Wolsey Shale, but the Fishtrap Formation has been interpreted as a return to a shallow marine to intertidal carbonate shelf (Harrison et al. 1986, Bush 1989).

BURIAL ALTERATION

Interpretation of ancient soil formation from paleosols requires geochemical and petrographic data in order to disentangle comparable alterations due to burial. Three burial diagenetic alterations of decomposition, gleization, and reddening common in paleosols (Retallack 2001) are evident from red beds of the Flathead Sandstone. Decomposition of organic matter is evident from the ferruginization of filamentous structures of presumed organic origin (Figs. 3H, 6B), which were originally part of the soil because they are truncated within redeposited soil clasts (Fig. 6D). Gleization of buried organic matter is indicated by green–gray haloes around fossil filaments of *Prasinema gracile* (Fig. 3F, G), which were presumably once carbonaceous and fueled local chemical reduction of their matrix after burial (Retallack 2011b). Burial gleization does not extend to whole horizons or form mottled horizons in red beds of the Flathead Sandstone, like it does in the Cambrian paleosols of South Australia (Retallack 2008). Burial reddening of the Flathead Sandstone also is likely due to common dehydration of ferric hydroxides because comparable coastal facies of Coos Bay, Oregon, are brown, not red (Nelson et al. 1996).

Ozkan and McBride (2007) determined from fluid inclusions of the Flathead Sandstone that its maximum temperature was 150 to 160° C during burial, and this reduced porosity to an average of 3.6% (range, 0–11.5%) and permeability to an average of 5.8 mD (range, 0.5–439 mD). Lebauer (1964) found that Wolsey Shale overlying the Flathead Sandstone was largely illite and poorly crystalline chlorite, without notable diagenetic alteration. Potash is high (up to 6.76 wt%) in these paleosols, but not because of potash metasomatism (Fedo et al. 1995), considering the molar losses from the Cool paleosol (Fig. 7). Rather, high-potash and little-weathered K-feldspars are well-known anomalies of Cambrian and Precambrian sediments, which reflect a different weathering regime before the advent of vascular land plants (Basu 1981, Retallack 2012b).

PALEOPEDOLOGY

Instead of a single strongly developed paleosol on top of the Belt Supergroup (Harrison et al. 1986), five successive paleosols were recognized from repeated patterns of grain size, color, and structures (Fig. 4). These initial field interpretations of Cambrian and Precambrian paleosols were then supported by laboratory studies of mineral and chemical composition, as detailed in the following paragraphs.

Paleosol Recognition

Within red siltstones of the Flathead Sandstone, weathered intervals (paleosol A horizons) are purple–red in color (Munsell weak red, 7.5R 4/2) and massive to hackly in appearance, whereas intervening sediments are planar bedded and purple–gray (Munsell dark reddish gray, 7.5R 4/1). The massive to hackly appearance corresponds to blocky to platy peds defined by argillans (in the terminology of soil science; Retallack 2001). These are irregular fractures lined with clay in thin section (Fig. 6E). In some cases the cracks are shallow, gaping, and coated with concentric ridges (Fig. 2G), as in polygonal oscillation cracks (Noffke 2010). In other cases, the fracturing is represented by more subtle seams of clay-lined rock.

Destruction of bedding is also the result of pervasive near-vertical filamentous structures of two distinct kinds: drab-haloed filament traces (Figs. 2G, 3F) and ferruginized-organic filaments (Fig. 3H). In thin section, the filaments are circular, as well as elliptical and elongate (Figs. 3F–H and 6A, B) and are oriented mainly vertical to bedding (all thin sections were cut in that orientation). The drab-haloed filament traces are similar to those described as *Prasinema gracile* from

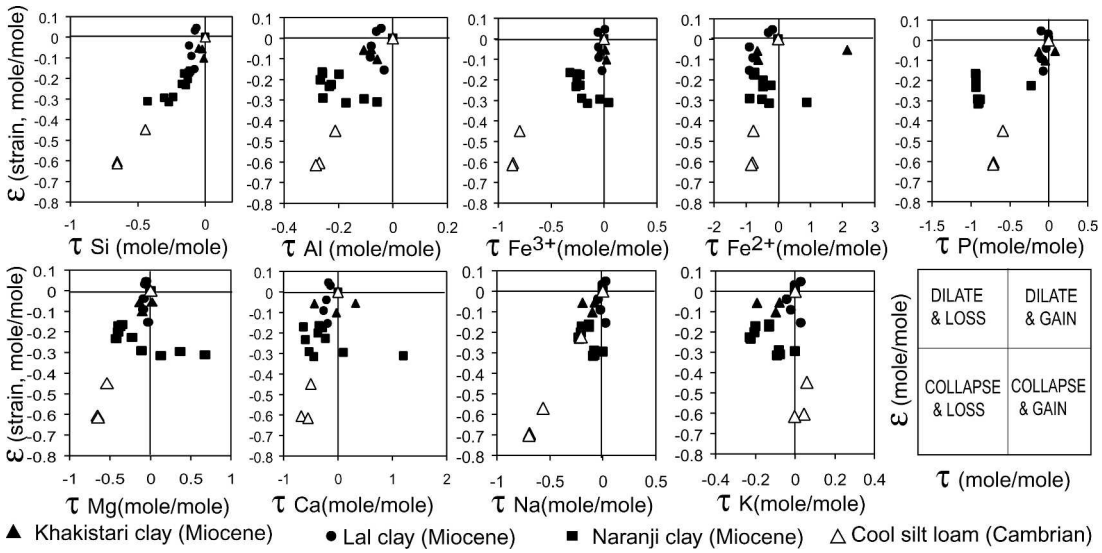

FIG. 7.—Mass balance geochemistry of Cool paleosol, including estimates of strain from changes in an element assumed stable (Ti) and elemental mass transfer with respect to an element assumed stable (Ti following Brimhall et al. [1992]) and by comparison with Miocene paleosols from Pakistan (Retallack 1991). Zero strain and mass transfer is the parent material lower in the profile: higher horizons deviate from that point as a result of pedogenesis.

Cambrian (Retallack 2008, 2011b) and Ordovician paleosols (Retallack 2009a, 2009b). Ferruginized filaments are ubiquitous and vary from 38 volume % in the surface (A) horizons to 12 volume % in subsurface (C) horizons (Table 1). These filaments are opaque and dominate the fabric of some thin sections (Fig. 6A, B), unlike intervening stratified sediments (Fig. 6C). Their vertical orientation and thorough admixture with mineral grains through a considerable thickness of rock are characteristic of microbial earth soils (Belnap et al. 2003) and paleosols (Retallack 2008, 2011b, 2012a). Intertidal microbial mats, in contrast, have a sharp contact with underlying sediment, few included grains, and are eroded as folded and planar flakes (Noffke 2010), not seen in the red beds of Radio Creek.

The filament-rich (A) horizons are also picked out by magnetic susceptibility peaks, in proportion to point-counted abundance of ferruginous filaments (Fig. 4). These data are discussed at length by Retallack et al. (2003), who conclude that they represent precipitation of iron minerals within the most microbially active portion of the paleosol. Only well-drained modern soils show such surficial increases in magnetic susceptibility, presumably because the microbes responsible are aerobic (Maher 1998, de Jong et al. 2000). In contrast, microbially induced magnetic susceptibility is destroyed in modern gleyed soils (Grimley and Vepraskas 2000) and paleosols (Retallack et al. 2003), so that peaks in susceptibility represent well-drained parts of these estuarine paleosols.

The filament-rich horizons also show petrographic evidence of significant weathering (depleted abundance of rock fragments, feldspar, and mica compared with lower horizons in Fig. 5). The ferruginized filament-rich upper parts of the paleosols are especially striking (Fig. 6B) in thin section, compared with the filament-poor lower parts of the paleosols (Fig. 6C), because clays associated with filaments are highly birefringent, a distinctive soil feature called "sepic plasmic fabric," created by the uniquely deviatoric local stresses of soil formation (Retallack 2001). The amount of birefingent clay is markedly greater in paleosol surface horizons than in their parent materials or associated sediments (Table 1). Additional evidence of weathering comes from chemical analysis showing peaks in barium/strontium and alumina/silica molar ratios indicative of leaching and clay formation at the surface of the paleosol (Fig. 5). A more comprehensive accounting of chemical weathering comes from analysis of strain and mass transfer (Eqs. 1, 2) in the basal Cool paleosol, formed on little weathered breccia of the Libby Formation (Fig. 5).

Assuming that the titania content of that breccia represents parent material, there was significant loss of mass (negative strain) due to weathering of the Cool paleosol (Fig. 7), in excess of the strain found in the Miocene woodland paleosols of Pakistan (Retallack 1991). In addition, like the Pakistani paleosols, the Cool paleosol lost silica, ferric iron, magnesia, lime, soda, and phosphorus, but it lost little potash. Chemical weathering of the Cool paleosol is strong, yet shallower than that noted in the Pakistani paleosols (Fig. 8), which are penetrated by fossil root traces to depths of up to 2.3 m (Retallack 1991). One of the Pakistani paleosols (Khakistari of Fig. 8) shows strong enrichment of ferrous iron at depth, attributed to original waterlogging (Retallack 1991), but comparable evidence of biological iron reduction was not found at any depth in the Cool paleosol. These strain and mass transfer relationships are only plausible in weathering environments, because sedimentary graded beds do not create surficial enrichment of titanium, which is in heavy minerals such as ilmenite, deposited as placers near the base of beds. In soils, however, titanium is enriched at the surface with weathering of other elements, particularly alkali and alkaline earths (Brimhall et al. 1992).

Pedotypes

The five successive paleosols of red beds of Radio Creek are of two distinct kinds, here designated "Radio" and "Cool" pedotypes, after the nearby creeks. A pedotype is a kind of paleosol defined on field characteristics and based on a type section (Retallack 1994).

The Radio pedotype at the top of the red beds has a surface (A) horizon that is red with drab-haloed filament traces (olive yellow 5Y 6/6 in matrix weak red 7.5R 4/1) above n horizon (Bg) with pyrite spherulites measuring 4 cm in diameter (Fig. 2D) and siderite nodules measuring 6 cm long in dark bluish-gray (5B 4/1) shale. Only one example of this kind of paleosol was seen.

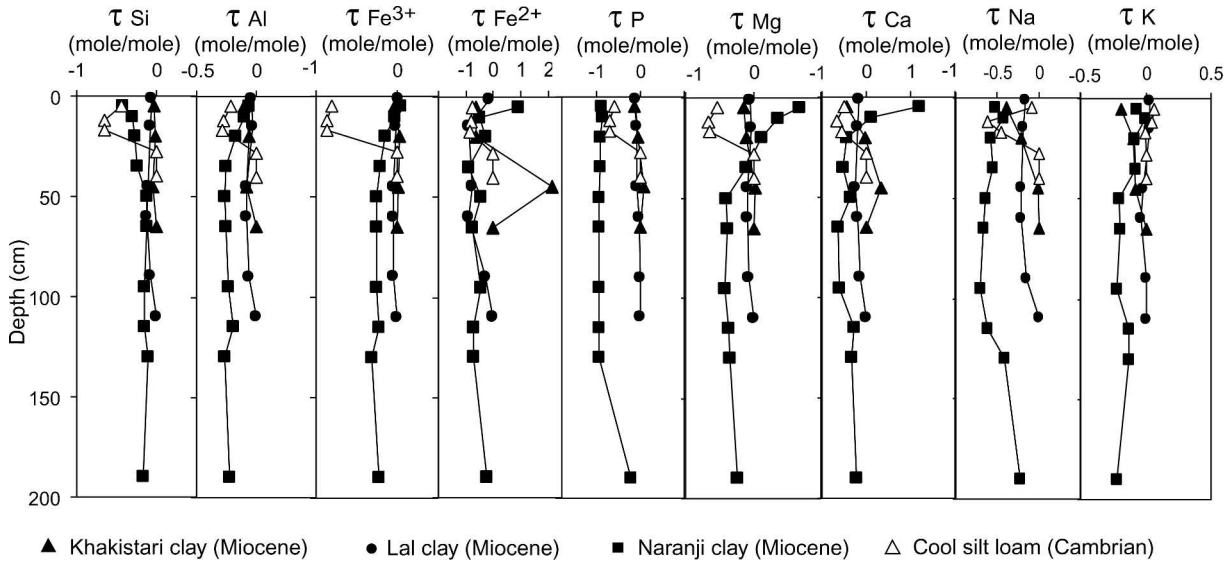

FIG. 8.—Mass transfer with depth in the Cool paleosol and some Miocene paleosols from Pakistan (Retallack 1991).

The Cool pedotype, in contrast, has a surface (A) horizon reddened (weak red 7.5R 4/2) with abundant hematite filaments and only scattered irregular drab (light greenish-gray 5GY 7/1) mottles, above subsurface (C) horizons of gray (5YR 5/1) micaceous siltstone. Most paleosols of the red beds of the Flathead Sandstone have this simple profile form and are developed on silty shale parent material, but the one here designated as the type profile was formed on gray claystone breccia at the base of the section (Fig. 4).

Comparable Paleosols

Cambrian paleosols from the Flinders Ranges of Australia (Retallack 2008) and the Cantabrian Mountains of Spain (Álvaro et al. 2003) are comparable with those of the Flathead Sandstone in Montana in their red color, hydrolytic weathering profiles, limited depth, and intensity of filaments and are also within sequences containing marine body and trace fossils in other beds. Both are also within thicker sedimentary sequences including fully marine limestones and fluvial sandstone paleochannels, which provide evidence of a wider range of marine to alluvial paleoenvironments. Cambrian paleosols of the Flathead Sandstone lack the large illuviation argillans and concretionary structures of the Spanish Cambrian paleosols, attributed to seasonal paleoclimate (Álvaro et al. 2003), and the micritic nodules of the Australian Cambrian paleosols, attributed to dry paleoclimate (Retallack 2008). All of these Cambrian paleosols also have fabrics dominated by drab-haloed and ferruginous filamentous structures, which are also known in red Neoproterozoic paleosols dating back to 1800 Ma (Driese et al. 1995, Mitchell and Sheldon 2009, Retallack 2011a).

Comparable Modern Soils

In modern soil taxonomy (Soil Survey Staff 2000), the Radio pedotype with its pyrite spherulites and relict bedding can be interpreted as a Sulfaquent, which is a gleyed sulfidic soil of weak development, usually marginal marine (Retallack 2001). The Cool pedotype, in contrast, can be interpreted to represent former Fluvent soils (Soil Survey Staff 2000). In the classification of the Food and Agriculture Organization (1974), the Radio pedotype was a Thionic Fluvisol (Jt) and the Cool pedotype a Dystric Fluvisol (Jd).

Comparable soilscapes are widespread in large tropical coastal estuaries (Food and Agriculture Organization 1971, 1977a, 1977b, 1979). Their coastal location occurs because marine sulfate is a prolific source of sulfides: freshwater does not contain suitable levels of sulfate (Altschuler et al. 1983, Bush et al. 2004). As can be seen from associated soils and soil inclusions in these map areas (Table 3), such soils are now limited to peaty mangrove and saltmarsh soils within deltas and estuaries. Large molluscs and a variety of vascular plants in such modern soils had not evolved by the Cambrian, when Thionic Fluvisols may have been more widespread in coastal regions. Coos Bay, Oregon, with a sedimentary environment comparable to that of the Flathead Sandstone, does not have Thionic Fluvisols because of high organic matter content under the salt marshes (Nelson et al. 1996), which also evolved after the Cambrian. Coos Bay estuary does have Dystric Fluvisols, or very weakly developed alluvial soils (Lund 1973), in areas too small to be featured on the Food and Agriculture Organization (1975) soil map.

Paleoclimate

Paleoprecipitation can be gained from paleosols using the paleohyetometer of Sheldon et al. (2002), based on chemical index of alteration without potash ($C = 100 \times mAl_2O_3/[mAl_2O_3 + mCaO + mNa_2O]$, in moles), which increases with mean annual precipitation (P, in mm) in modern soils ($R^2 = 0.72$; standard error [SE] = ±182 mm), as follows:

$$P = 221e^{0.0197C}. \quad (3)$$

This formulation is based on the hydrolysis equation of weathering, which enriches alumina at the expense of lime, magnesia, potash, and soda. Magnesia is ignored because it is not significant for most sedimentary rocks, and potash is excluded because it can be enriched during deep burial alteration of sediments (Fedo et al. 1995, Sheldon and Tabor 2009). A useful paleotemperature proxy for paleosols devised by Sheldon et al. (2002) is alkali index ($N = [K_20 + Na_2O)/Al_2O_3]$, as a molar ratio), which is related to mean annual temperature (T, in ° C) in modern soils by Eq. 4 ($R^2 = 0.37$; SE = ±4.4° C):

TABLE 3.—Modern distribution of Thionic Fluvisol (Jt) soils.*

Map symbol	Associated soils	Inclusions	Area (ha × 10^3)	Nearest town	Geomorphic area	Country	Year
Jt-12–3a	Od	Gd, R, P	281	Buntui	Sebangan Bay	Kalimantan	1979
Jt-12–3a	Od	Gd, R, P	53	Mempakul	Brunei Bay	Sarawak	1979
Jt-12–3a	Od	Gd, R, P	400	Beluran	Marchesa Bay	Sabah	1979
Jt-13–3a		Gh	1119	Chi Phu	Mekong Delta	Vietnam	1979
Jt-13–3a		Gh	222	Kompong Som	Kompong Bay	Kampuchea	1979
Jt-14–3a	Gh	Gd	1424	Pathum Thani	Chao Phraya River	Thailand	1979
Jt-14–3a	Gh	Gd	531	Mac Bai	Mekong Delta	Vietnam	1979
Jt-14–3a	Gh	Gd	427	Kuantan	Pahang River	Malaysia	1979
Jt10-3a	Jc, Zg	O	538	Amtali	Bay of Bengal	Bangladesh	1977b
Jt10-3a	Jc, Zg	O	574	Kakdwip	Hoogli River	India	1977b
Jt11-3a		Zg	756	Bogale	Irrawaddy Delta	Myanmar	1977b
Jt1-3a	Zg, Rd, Ph	Ao	183	Maraú	Ponta do Muta	Brazil	1971
Jt2–1/2a	Zg	Re	150	Banjul	Pointe de Sangomar	Gambia	1977a
Jt2–1/2a	Zg	Re	165	Kaolack	Saloume Delta	Senegal	1977a
Jt2-2a	Zg	Re	240	Nouâdibou	Arguin Gulf	Mauritania	1977a
Jt2-3a	Zg		294	Ziguinchor	Casamance Delta	Senegal	1977a
Jt3-2a	Zg		585	Bissau	Geba River	Guinea-Bissau	1977a
Jt3-2a	Zg		194	Varela	Cacheu River	Guinea-Bissau	1977a
Jt4-a	Gh, Zg		1225	Nembe	Niger Delta	Nigeria	1977a
Jt4-2a	Gh, Zg		307	Gbanbatok	Sherbro River	Sierra Leone	1977a
Jt5-3a	O, Zg		525	Boke	Nunez River	Guinea	1977a
Jt6-3a			85	Vilanculos	Cape São Sebastião	Mozambique	1977a
Jt7-3a		Jd, Je	32	Kionga	Ruvuma River	Tanzania	1977a
Jt8-2a	Jc, Zg	Gc, Z	1287	Soalala	Cape Saint André	Madagascar	1977a

* Year is the publication date of the soil map reference citation for the Food and Agriculture Organization: Soil abbreviations include the following: Ao, Orthic Acrisol; Gd, Dystric Gleysol; Gh, Humic Gleysol; Jc, Calcaric Fluvisol; Je, Eutric Fluvisol; Jt, Thionic Fluvisol; O, Histosol; Od, Dystric Histosol; P, Podzol; Ph, Humic Podzol; R, Regosol; Rd, Dystric Regosol; Re, Eutric Regosol; Zg, Gleyic Solonchak.

$$T = -18.5N + 17.3. \quad (4)$$

Both of these proxies are derived from chemical analyses of North American soils, not including intertidal soils, but there are modern coastal soils in the training set (Sheldon et al. 2002), and that is why this technique was applied only to the lowest and most inland of the Cool paleosols developed on the basal breccia of the Flathead Formation (Fig. 4). Application of these chemical proxies to the most deeply weathered subsurface horizon of the type Cool paleosol yields a tropical humid climate: mean annual precipitation measures 1502 ± 182 mm, and mean annual temperature measures 17 ± 4.4° C. The Cool paleosol also has elevated barium:strontium and alumina:silica ratios (Fig. 5), in support of such a warm, humid paleoclimate. The quartz-rich composition of Flathead Sandstone (Fig. 6F) also provides evidence of profound chemical weathering.

Another indication of humid paleoclimate is lack of evaporites in the paleosols of Radio Creek. Semiarid Cambrian paleosols of South Australia include common gypsum and halite crystals and pseudomorphs (Retallack 2008). Lack of evaporites is another similarity between paleosols of Radio Creek and modern estuarine to deflation plain soils of humid Coos Bay, Oregon (Lund 1973, Nelson et al. 1996). Warm, humid paleoclimate is compatible with the near-equatorial (ca. 10° S) location of this part of Laurentia at the Cambrian–Precambrian boundary (Meert and Lieberman 2001). Chinese characters selected for euphony and felicity for the Cambrian Period ("Hanwu Ji") also mean, in other contexts, "fierce cold" (Brasier 1992), and there is now supporting evidence for widespread glaciation in Avalonia, Kyrgyzstan, Siberia, and China during the latest Ediacaran and Early Cambrian (Chumakov 2007, 2011; Landing and McGabhann 2010). Such frigid climates are unlikely to have extended to equatorial regions, but there is also evidence from time series of paleosols in South Australia (Retallack 2008, 2009a) and Spain (Álvaro et al. 2003) that the earliest Cambrian paleosols formed under a wetter and warmer paleoclimate than did Late Ediacaran and succeeding Early Cambrian paleosols.

Former Ecosystem

Both Cool and Radio paleosols contain abundant ferruginous filaments (Table 4), which are copiously branched and near-circular in cross section (Figs. 3G, H and 6A, B, D), comparable with those found in other Cambrian paleosols (Álvaro et al. 2003). These filaments are Cambrian in age because they were found within redeposited clasts of the paleosols (Figs. 5E, 6D). Some of these filaments also have drab haloes (Fig. 2F), like *Prasinema gracile* (Retallack 2011b), attributed to burial gleization of remnant organic filaments in Cambrian paleosols (Retallack 2008). Where ferruginized filaments are abundant, magnetic susceptibility is high, and where drab-haloed filaments are abundant, magnetic susceptibility is low (Fig. 3). These are also patterns of magnetic susceptibility created by soil microbes in well-drained and poorly drained modern soils, respectively (Retallack et al. 2003). Activity of organic ligands from microbes can be inferred from chemical weathering, especially phosphorus depletion (Neaman et al. 2005), which was marked in the Cool paleosol (Figs. 7, 8).

The morphology of the filamentous structures is comparable with microbial filaments in biological soil crusts of modern deserts (Belnap

TABLE 4.—Diagnosis, classification, and interpretation of Cambrian pedotypes.

Pedotype	Radio	Cool
Source of name	Radio Creek, outlet for Fishtrap Lake	Cool Creek into Fishtrap Lake
Diagnosis	red massive silty surface (A) over sideritic nodular and pyritic red siltstone (Bg) and bedded siltstone (C)	red massive siltstone (A) over bedded red siltstone (C)
US taxonomy	Sulfaquent	Fluvent
FAO soil type	Thionic Fluvisol	Dystric Fluvisol
Paleoclimate	not diagnostic for paleoclimate	humid (mean annual precipitation 1502 ± 182 mm) tropical (mean annual temperature 17 ± 4.4° C)
Paleoecosystem	microbial polsterland	microbial polsterland
Paleotopography	lagoonal supratidal flats	estuarine supratidal flats
Parent material	quartzofeldspathic silt	quartzofeldspathic silt and breccia
Time for formation	1–3 kyrs	1–3 kyrs

FAO = Food and Agriculture Organization.

et al. 2003). These Cambrian paleosols may have been microbial earths, as defined by Retallack (1992), but scattered megascopic filament bundles (now drab-haloed) indicate polsterlands of microbial consortia such as lichens and bacterial colonies. Depletion of original organic matter by ferruginization and local gleization makes it unlikely that the biological identity of these microbes will be decipherable. Perhaps they included *Leptothrix* or comparable iron-fixing bacteria, as suggested for Cambrian paleosols by Álvaro et al. (2003). *Microcoleus* or comparable rope-forming cyanobacteria are also a possibility, as suggested for Cambrian paleosols by Retallack (2008). The presumed marine invertebrates responsible for local trace fossils (Fig. 3) would have been sustained by microbial and other particulate organic matter in water, perhaps in part derived from these local estuarine soils.

Parent Materials

Common rounded sand grains of silty Libby Formation in the parent material of Cool paleosols and a basal unconformity littered with breccia of Libby Formation clasts are evidence that these rocks were lithified and formed the immediate source area for red beds of the Flathead Sandstone. Such rock fragments are found in most of the paleosols, and dominance of mineral composition by quartz and feldspar (Fig. 4) is an indication that similar rocks were widespread in the source terrane. There is more feldspar than quartz in most of the paleosols, but not in the Flathead Sandstone (Table 1; Fig. 4), which may include material from a much wider region (Oksan and McBride 2007). Persistence of feldspar in Early Paleozoic and Precambrian sandstones has been attributed to a less intense weathering regime before evolution of vascular land plants (Basu 1981, Dott 2003), but the Cool paleosol, which retained potash, was more intensely weathered than are the Miocene paleosols (Fig. 7). In addition, potash retention is not due to unusually alkaline Early Paleozoic groundwater (Jutras et al. 2009), because other bases are profoundly depleted in the Cool paleosol (Figs. 7, 8). Conservation of potash, as seen in the Cool paleosol (Figs. 7, 8), is widespread in Precambrian paleosols dating back 2.6 Ga (Driese et al. 1995, Watanabe et al. 2000). Potash-rich composition of pre-Silurian paleosols and their parent materials may be due to biological selectivity of cations under microbial communities with nutrient demands different from those of vascular land plants (Basu 1981).

Paleotopography

The shallow depth of ferruginization and of surface brecciation and mud cracks in these paleosols (Figs. 2G, 4) offers evidence of a water table generally located within 30 cm of the surface, as in modern estuarine, lakeshore, or floodplain soils (Vepraskas and Sprecher 1991). Ubiquitous planar bedding in their silty parent materials is also evidence of a sedimentary environment of low topographic relief, similar to the barrier bar and tidal flats of modern Coos Bay, Oregon (Lund 1973, Nelson et al. 1996). Thickness variations in red beds of the Flathead Sandstone have been mapped at 0 to 6 m (Fig. 1) and are interpreted to represent infill of paleotopography overriden by barrier bar sandstones. Thus, the bedrock cliffs flanking the estuary had at least 6 m of local topographic relief.

Time for Formation

Modern soils with shallow relict bedding like Cool and Radio paleosols form over periods of a few to several hundreds of years (Nelson et al. 1996). Roots of salt marsh and mangal plants and burrows of worms and molluscs accelerate physical weathering in structurally comparable modern soils (Oglesby 1973, McCauley et al. 1977), but the chemical differentiation of the Radio and Cool paleosols indicates longer times for formation. Siderite nodules measuring up to 6 cm in length and pyrite spherulite casts up to 4 cm in diameter in the Radio paleosol are evidence of chemical differentiation of a gleyed horizon (Bg of Soil Survey Staff [2000]). Siderite nodules of comparable size enclosing crab and yabbie fossils are found in tropical estuarine soils of Australia within the intertidal range, so they are likely Late Holocene in age (Etheridge and McCulloch 1916). Siderite nodules measuring up to 1 cm in diameter were found in core of a marsh soil at a level younger than 680 ± 40 radiocarbon years in Loboi Swamp, Kenya (Ashley et al. 2004). Common (ca. 4 wt % reduced S) microscopic (<5-μm) marcasite platelets formed during an interval of vegetation change of less than 1000 years after 4704 ± 70 radiocarbon years in Bungawalbin Swamp, New South Wales (Bush et al. 2004). Thus, many centuries may be needed to form nodules and spherulites as large as those in the Radio paleosol. Chemical weathering of the Cool paleosol is greater than that seen in Miocene swamp and woodland soils thought to have formed over as many as 10,000 years (Retallack 1991). Chemical rather than physical weathering of these Cambrian paleosols may be a better guide to their times of formation, which are likely to have been several thousand years.

CONCLUSIONS

Paleosols and sedimentary paleoenvironment of red beds of the Flathead Sandstone are reconstructed in Figure 9 and summarized in Table 4. The basal Cambrian paleosols of Montana are comparable to other Cambrian and Proterozoic red paleosols (Driese et al. 1995; Retallack 2008, 2011a; Mitchell and Sheldon 2009) in showing simple

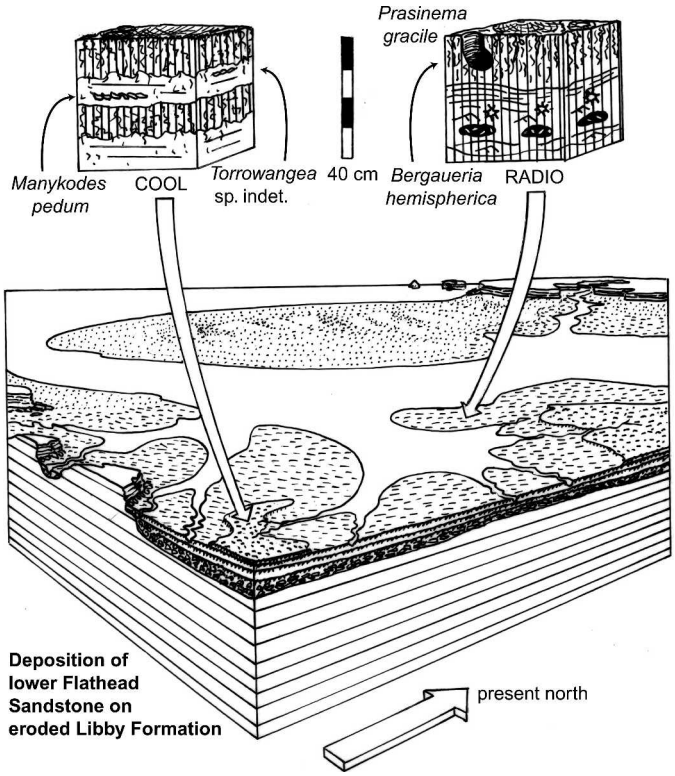

FIG. 9.—Reconstructed basal Cambrian paleoenvironment of the lower Flathead Sandstone near Fishtrap Lake, Montana.

A–Bg–C or A–C profiles, with abundant filamentous bioturbation of presumed microbial origin and substantial chemical weathering, especially of phosphorus, which is also likely to have been biologically mediated (Neaman et al. 2005). These living soils were not far from the ocean, based on sedimentary similarities of the Flathead Sandstone and barrier bars and rock-bound estuaries (Lund 1973). Marine-influenced parent materials to the paleosols include a suite of marine trace fossils (*Bergaueria hemispherica*, *Didymaulichnus lyelli*, *Torrowangea* sp. indet., *Manykodes pedum*), which fix the age of these paleosols as very Early Cambrian (Fortunian; Landing et al. 2007). The degree of chemical weathering of one of the paleosols (type Cool profile) is evidence of a tropical humid climate, which is compatible both with an equatorial paleolatitude of this part of Laurentia during the earliest Cambrian (Meert and Lieberman 2004) and with evidence from other paleosol sequences that the earliest Cambrian was unusually warm and wet compared with the Ediacaran and later Early Cambrian (Retallack 2008).

Recognition of Cambrian paleosols is based on disruption of primary sedimentary structures (ripple marks, planar bedding) and imposition of soil structures (blocky peds, filamentous structure, pyrite spherulites, siderite nodules), but Cambrian soil formation was not so deep or pervasive as in paleosols after the Devonian evolution of trees and their distinctive large rooting structures (Driese et al. 1997, Driese and Mora 2001, Retallack and Huang 2011). Thus, indications of physical weathering need to be supplemented by analysis of chemical weathering, which in these Early Cambrian paleosols is surprisingly profound, though still shallow in depth, compared with geologically younger soils and paleosols. Hydrolytic base depletion is demonstrated here, but Cambrian paleosols are more like Precambrian profiles than modern soils in retaining potash. The soil-forming process of gleization is also demonstrated with the growth of gley minerals (pyrite and siderite) in less organic paleosols than the soils in which these minerals are found today (Ashley et al. 2004, Bush et al. 2004). Cambrian soil formation was similar in outline to modern soil formation, but notable differences reflect differences in their biota.

ACKNOWLEDGMENTS

Mark Storaasli discovered the locality at Fishtrap Lake and collected important fossils. Nicholas and Jeremy Retallack and Dmitri Grazhdankin helped during fieldwork. Bruce Runnegar, Shuhai Xiao, and Bill Schopf offered useful discussion. The manuscript was greatly improved by the perceptive reviews of Nora Noffke, Tony Runkel, Steven Driese, and Lee Nordt.

REFERENCES

Aadland RK. 1985. Lithofacies of the Middle-Upper Cambrian Sequence, Libby Syncline, Montana: Montana Bureau of Mines and Geology, Butte. Open-File Report, 80 p.

Aarseth I, Fossen H. 2004. A Holocene lacustrine rock platform around Storavatnet, Osteroy, western Norway. *Holocene* 14:589–596.

Altschuler ZS, Schnepfe MM, Silber CC, Simon FO. 1983. Sulfur diagenesis in Everglades peat and the origin of pyrite in coal. *Science* 221:221–227.

Álvaro JJ, van Vliet-Lanoë B, Vennin E, Blanc-Valleron MM. 2003. Lower Cambrian paleosols from the Cantabrian Mountains (northern Spain): a comparison with Neogene–Quaternary estuarine analogs. *Sedimentary Geology* 163:67–84.

Armentrout JM. 1981. Cenozoic stratigraphy of Coos Bay and Cape Blanco, southwestern Oregon. *In* Oles KF, Johnson JG, Niem AR, Niem WA (Editors). *Geologic Field Trips in Western Oregon and Southwestern Washington*, Bulletin 101: Oregon Department of Geology and Mineral Industries, Portland. p. 175–216.

Ashley GM, Maitima Mworia J, Muasya AM, Owen RB, Driese SG, Hover CV, Renaut RW, Goman WF, Mathai S, Blatt SH. 2004. Sedimentation and recent history of a freshwater wetland in a semiarid environment: Loboi Swamp, Kenya, East Africa. *Sedimentology* 51:1301–1321.

Bannister FA. 1932. The distinction of pyrite from marcasite in nodular growths. *Mineralogical Magazine* 23:179–187.

Basu A. 1981. Weathering before the advent of land plants: evidence from unaltered K-feldspars in Cambrian–Ordovician arenites. *Geology* 9:132–133.

Belnap J, Büdel B, Lange OL. 2003. Biological soil crusts: characteristics and distribution. *In* Belnap J, Lange OM (Editors). *Biological Soil Crusts: Structure, Function and Management*: Springer, Berlin. p. 3–30.

Brasier MD. 1992. Global ocean–atmosphere change across the Precambrian–Cambrian transition. *Geological Magazine* 129:161–168.

Brimhall GH, Chadwick OA, Lewis CJ, Compston W, Williams IS, Danti KJ, Dietrich WE, Power ME, Hendricks D, Bratt J. 1992. Deformational mass transport and invasive processes in soil evolution. *Science* 255:695–702.

Buatois L, Mángano MG. 2011. *Ichnology: Organism–Substrate Interactions in Space and Time*: Cambridge University Press, Cambridge, UK. 358 p.

Bush JH. 1989. The Cambrian System of northern Idaho and northwestern Montana. *In* Chamberlain VE, Breckenridge RM, Bonnichsen B (Editors). *Guidebook to the Geology of Northern and Western Idaho and Surrounding Area*, Bulletin 19: Idaho Bureau of Mines and Geology, Moscow. p. 103–121.

Bush RT, McGrath R, Sullivan LA. 2004. Occurrence of marcasite in an organic-rich Holocene mud. *Soil Research* 42:617–621.

Chaudhuri S, Brookins DG. 1969. The isotopic age of the Flathead Sandstone (Middle Cambrian), Montana. *Journal of Sedimentary Petrology* 39:364–366.

Chumakov NM. 2007. Climates and climate zonality of the Vendian: geological evidence. *In* Vickers-Rich P, Komarower P (Editors). *The Rise and Fall of the Ediacaran Biota*, Special Publication 286: Geological Society London. p. 15–26.

Chumakov NM. 2011. Late Proterozoic African glacial era. *Stratigraphy and Geological Correlation* 19:1–20.

Cloud P. 1973. Pseudofossils; a plea for caution. *Geology* 1:123–127.

Colpron M, Logan JM, Mortensen JK. 2002. U-Pb zircon age constraint for Late Neoproterozoic rifting and initiation of the lower Paleozoic passive margin of western Laurentia. *Canadian Journal of Earth Sciences* 39:133–143.

Cowan CA, James NP. 1992. Diastasis cracks; mechanically generated synaeresis-like cracks in Upper Cambrian shallow water oolite and ribbon carbonates. *Sedimentology* 39:1101–1118.

Crimes TP, Legg I, Marcos A, Arboley M. 1977. ?Late Precambrian–low Lower Cambrian trace fossils from Spain. *In* Crimes TP, Harper JC (Editors). Trace fossils 2. *Geological Journal Special Issue* 9:91–138.

Daily B, Moore PS, Rust BR. 1980. Terrestrial–marine transition in the Cambrian rocks of Kangaroo Island, South Australia. *Sedimentology* 27:379–399.

Davies NS, Gibling MR. 2010. Paleozoic vegetation and the Siluro–Devonian rise of fluvial lateral accretion sets. *Geology* 38:51–54.

Davies NS, Gibling MR, Rygel MC. 2011. Alluvial facies evolution during the Palaeozoic greening of the continents: case studies, conceptual models and modern analogues. *Sedimentology* 58:220–258.

de Jong E, Pennock DJ, Nestor PA. 2000. Magnetic susceptibility of soils in different slope positions in Saskatchewan, Canada. *Catena* 40:291–305.

Dott RH. 2003. Importance of eolian abrasion in supermature quartz sandstone and the paradox of weathering in vegetation-free landscapes. *Journal of Geology* 111:387–405.

Driese SG, Mora CI. 2001. Diversification of Siluro–Devonian plant traces in paleosols and influence on estimates of paleoatmospheric CO_2 levels. *In* Gensel PG, Edwards D (Editors). *Plants Invade the Land: Evolutionary and Environmental Perspectives*: Columbia University Press, New York. p. 237–253.

Driese SG, Mora CI, Elick JM. 1997. Morphology and taphonomy of root and stump casts of the earliest trees (Middle to Late Devonian), Pennsylvania and New York, USA. *Palaios* 12:524–537.

Driese SG, Simpson EL, Eriksson KA. 1995. Redoximorphic paleosols in alluvial and lacustrine deposits, 1.8 Ga Lochness Formation, Mount Isa, Australia; pedogenic processes and implications for paleoclimate. *Journal of Sedimentary Research* A65:675–689.

Droser ML, Jensen S, Gehling JG, Myrow PM, Narbonne GM. 2002. Lowermost Cambrian ichnofabrics from the Chapel Island Formation, Newfoundland: implications for Cambrian substrates. *Palaios* 17:3–15.

Dzik J. 2005. Behavioral and anatomical unity of the earliest burrowing animals and the cause of the "Cambrian explosion." *Paleobiology* 31:503–521.

Ekdale AA, Lewis DW. 1991. Trace fossils and paleoenvironmental control of ichnofacies in a Late Quaternary gravel and loess fan delta complex, New Zealand. *Palaeogeography, Palaeoclimatology, Palaeoecology* 81:253–279.

Etheridge R, McCulloch AR. 1916. Sub-fossil crustaceans from the coasts of Australia. *Australian Museum Records* 11:1–14.

Evans KV, Aleinikoff JN, Obradovich JD, Fanning CM. 2000. SHRIMP U-Pb geochronology of volcanic rocks, Belt Supergroup, western Montana: evidence for rapid deposition of sedimentary strata. *Canadian Journal of Earth Sciences* 37:1287–1300.

Fedo CM, Nesbitt HW, Young GM. 1995. Unraveling the effects of potassium metasomatism in sedimentary rocks and paleosols, with implications for paleoweathering conditions and provenance. *Geology* 23:921–924.

Fedonkin MA. 1985. Paleoichnology of Vendian Metazoa. *In* Sokolov BS, Iwanowski AB (Editors). *The Vendian System*, Vol. 1, *Paleontology*: Springer, Berlin. p. 132–137.

Food and Agriculture Organization. 1971. *Soil Map of the World*, Vol. 4: *South America*: United Nations Educational and Scientific Organization, Paris. 193 p.

Food and Agriculture Organization. 1974. *Soil Map of the World*, Vol. 1: *Legend*: United Nations Educational and Scientific Organization, Paris. 59 p.

Food and Agriculture Organization. 1975. *Soil Map of the World*, Vol. 2: *North America*: United Nations Educational and Scientific Organization, Paris. 210 p.

Food and Agriculture Organization. 1977a. *Soil Map of the World*, Vol. 6: *Africa*: United Nations Educational and Scientific Organization, Paris. 299 p.

Food and Agriculture Organization. 1977b. *Soil Map of the World*, Vol. 7: *South Asia*: United Nations Educational and Scientific Organization, Paris. 117 p.

Food and Agriculture Organization. 1979. *Soil Map of the World*, Vol. 9: *Southeast Asia*: United Nations Educational and Scientific Organization, Paris. 149 p.

Frankel KL, Pazzaglia FJ, Vaughn JD. 2007. Knickpoint evolution in a vertically bedded substrate, upstream-dipping terraces, and Atlantic slope bedrock channels. *Geological Society of America Bulletin* 119:476–486.

Gehling JG, Jensen S, Droser ML, Myrow PM, Narbonne GM. 2001. Burrowing below the basal Cambrian GSSP, Fortune Head, Newfoundland. *Geological Magazine* 138:213–218.

Geyer G, Uchman A. 1995. Ichnofossil assemblages from the Nama Group (Neoproterozoic–Lower Cambrian) in Namibia and the Proterozoic–Cambrian boundary problem revisited. *Beringeria Special Issue* 2:175–202.

Gradstein FM, Ogg JG, Smith AG. 2004. *A Geologic Time Scale 2004*: Cambridge University Press, Cambridge, UK. 589 p.

Grazhdankin D, Krayushkin AV. 2007. Trace fossils and the upper Vendian boundary in the southeastern White Sea region. *Doklady Earth Sciences* 416:1027–1031.

Greb SF, Archer AW. 1995. Rhythmic sedimentation in a mixed tide and wave deposit, Hazel Patch Sandstone (Pennsylvanian), eastern Kentucky coal field. *Journal of Sedimentary Research* B65:96–106.

Grimley DA, Vepraskas MJ. 2000. Magnetic susceptibility for use in delineating hydric soils. *Soil Science Society of America Journal* 64:2174–2180.

Hagadorn JW, Bottjer DJ. 1997. Wrinkle structures; microbially mediated sedimentary structures common in subtidal siliciclastic settings at the Proterozoic–Phanerozoic transition. *Geology* 25:1047–1050.

Hagadorn JW, Collett JH, Belt ES. 2011a. Eolian–aquatic deposits and faunas of the Middle Cambrian Potsdam Group, New York. *Palaios* 26:314–334.

Hagadorn JW, Kirschvink JL, Raub TB, Rose EC. 2011b. Above the great unconformity: a fresh look at the Tapeats Sandstone Arizona–Nevada, USA. *Museum of Northern Arizona Bulletin* 67:63–77.

Hall J. 1852. *Palaeontology of New York*: C. van Benthuysen, New York. 362 p.

Häntzschel W. 1975. *Treatise on Invertebrate Paleontology*, Part W, Miscellanea. Supplement 1. *Trace Fossils and Problematica*: Geological Society of America, Boulder, Colorado. 269 p.

Harrison JE, Griggs AB, Wells JD. 1986. Geologic and Structure Maps of the Wallace 1°x2° Quadrangle, Montana and Idaho: US Geological Survey Miscellaneous Publications, Vol. I-1509A, 1 p.

Illich HA, Hall FW, Alt D. 1972. Ice-cemented sand blocks in the Pilcher Quartzite, western Montana. *Journal of Sedimentary Petrology* 42:927–929.

Jensen S. 1997. *Trace Fossils from the Lower Cambrian Mickwitzia Sandstone, South-Central Sweden*, Fossils and Strata 42: Scandinavian University Press, Oslo, Norway. 111 p.

Jensen S, Droser ML, Gehling JG. 2006. A critical look at the Ediacaran trace fossil record. *In* Xiao S, Kaufman AJ (Editors). *Neoproterozoic Geobiology and Paleobiology*: Springer, New York. p. 115–157.

Jensen S, Gehling JG, Droser ML. 1998. Ediacara-type fossils in Cambrian sediments. *Nature* 393:567–569.

Jensen S, Mens K. 2001. Trace fossils *Didymaulichnus* cf. *tirasensis* and *Monomorphichnus* isp. from the Estonian Lower Cambrian, with a discussion on the Early Cambrian ichnocoenoses of Baltica. *Estonian Academy of Sciences Proceedings Geology* 50:75–85.

Jensen S, Palacios T, Marti Mus M. 2007. A brief review of the fossil record of the Ediacaran–Cambrian transition in the area of Montos de Toledo—Guadalupe, Spain. *In* Vickers-Rich P, Komarower P (Editors). *The Rise and Fall of the Ediacaran Biota*, Special Publication 286: Geological Society London. p. 223–235.

Jensen S, Runnegar BN. 2005. A complex trace fossil from the Spitzkop Member (terminal Ediacaran–?Lower Cambrian) of southern Namibia. *Geological Magazine* 142:561–569.

Jutras P, Quillan RS, Le Forte MJ. 2009. Evidence from Middle Ordovician paleosols for the predominance of alkaline groundwater at the dawn of land plant radiation. *Geology* 37:91–94.

Keim JW, Rector RJ. 1964. Paleozoic rocks in northwestern Montana—a newly recognized occurrence. *Geological Society of America Bulletin* 75:575–578.

Klein G de V. 1970. Tidal origin of a Precambrian quartzite; the Lower Fine-grained Quartzite (Middle Dalradian) of Islay, Scotland. *Journal of Sedimentary Petrology* 40:973–985.

Kumpulainen RA, Uchman A, Woldehaimanot B, Kreuser T, Ghirmay S. 2006. Trace fossil evidence from the Adigrat Sandstone for an Ordovician glaciation in Eritrea, NE Africa. *Journal of African Earth Sciences* 45:408–420.

Landing E, McGabhann BA. 2010. First evidence for Cambrian glaciation

provided by sections in Avalonian New Brunswick and Ireland: additional data for Avalon–Gondwana separation by the earliest Palaeozoic. *Palaeogeography, Palaeoclimatology, Palaeoecology* 285:174–185.

Landing E, Narbonne GM, Myrow P, Benus AP, Anderson MM. 1988. Faunas and deposition environments of the Upper Precambrian through Lower Cambrian. *In* Landing E, Narbonne GM, Myrow P (Editors). Trace fossils, small shelly fossils and the Precambrian-Cambrian boundary: *New York State Museum Bulletin* 463:17–26.

Landing E, Peng S-C, Babcock LE, Geyer G, Moczydlowska-Vidal M. 2007. Global standard stages for the Lowermost Cambrian Series and Stage. *Episodes* 30:287–289.

Lebauer LR. 1964. Petrology of the Middle Cambrian Wolsey Shale of southwestern Montana. *Journal of Sedimentary Petrology* 34:503–511.

Leszcyński S. 2004. Bioturbation structures of the Kropivik Fucoid Marls (Campanian–lower Maastrichtian) of the Huwniki–Rybotycze area (Polish Carpathians). *Geological Quarterly Krakow* 48:35–60.

Lund EH. 1973. Oregon coastal dunes between Coos Bay and Sea Lion Point. *Ore Bin* 35:73–92.

Lund K, Aleinikoff JN, Evans KV, Fanning CM. 2003. SHRIMP U-Pb geochronology of Neoproterozoic Windermere Supergroup, central Idaho; implications for rifting of western Laurentia and synchroneity of Sturtian glacial deposits. *Geological Society of America Bulletin* 115:349–372.

Maher BA. 1998. Magnetic properties of modern soils and Quaternary loessic paleosols: paleoclimatic implications. *Palaeogeography, Palaeoclimatology, Palaeoecology* 137:25–54.

Martinsson A. 1970. Toponomy of trace fossils. *Geological Journal Special Issue* 3:323–330.

Mata S, Bottjer D. 2009. The paleoenvironmental distribution of Phanerozoic wrinkle structures. *Earth Science Reviews* 96:181–195.

McCauley JE, Parr RA, Hancock DR. 1977. Benthic infauna and maintenance dredging: a case study. *Water Research* 11:233–242.

Meert JG, Lieberman BS. 2004. A palaeomagnetic and palaeobiogeographical perspective on Neoproterozoic and Early Cambrian tectonic events. *Geological Society of London Journal* 161:477–487.

Mitchell RL, Sheldon ND. 2009. Weathering and paleosol formation in the 1.1 Ga Keweenawan Rift. *Precambrian Research* 168:271–283.

Moore PS. 1990. Origin of redbeds and variegated sediments, Cambrian, Adelaide Geosyncline, South Australia. *In* Jago JB, Moore PS (Editors). *The Evolution of a Late Precambrian–Early Palaeozoic Rift Complex: The Adelaide Geosyncline*, Special Publication 16: Geological Society of Australia, Sydney. p. 334–350.

Mukherji KK, Chakrabarti A, Roychaudiri S, Sarker S, Banerjee I. 1994. Herringbone cross stratification in environmental interpretation: a re-evaluation. *Indian Journal of Geology* 66:45–55.

Neaman A, Chorover J, Brantley SL. 2005. Element mobility patterns record organic ligands in soils on early Earth. *Geology* 33:117–120.

Nelson AR, Jennings AE, Kashima K. 1996. An earthquake history derived from stratigraphic and microfossil evidence of relative sea-level change at Coos Bay, southern coastal Oregon. *Geological Society of America Bulletin* 108:141–154.

Nelson WH, Dobell JP. 1961. Geology of the Bonner Quadrangle, Montana. *US Geological Survey Bulletin* 1111F:189–235.

Newton RS. 1968. Internal structure of wave formed ripple marks in the nearshore zone. *Sedimentology* 11:275–292.

Noffke N. 2010. *Geomicrobiology: Microbial Mats in Sandy Deposits from the Archean Era to Today*: Springer, Berlin. 194 p.

Oglesby LC. 1973. Salt and water balance in lugworms (Polychaeta: Arenicolidae), with particular reference to *Abarenicola pacifica* in Coos Bay, Oregon. *Biological Bulletin* 145:180–199.

Ohmoto H. 1996. Evidence in pre-2.2 Ga paleosols for the early evolution of atmospheric oxygen and terrestrial biota. *Geology* 24:1135–1138.

Ollier C, Pain C. 1996. *Regolith Soils and Landforms*: Wiley, Chichester, UK. 316 p.

Ozkan A, McBride EF. 2007. Diagenesis and porosity of the Flathead Sandstone (Middle Cambrian), Wyoming and Montana: American Association of Petroleum Geologists Annual Convention Abstracts, p. 105.

Pemberton SG, Frey RW, Bromley RG. 1988. The ichnotaxonomy of *Conostichus* and other plug-shaped ichnofossils. *Canadian Journal of Earth Science* 25:866–892.

Pemberton SG, Magwood JPA. 1990. A unique occurrence of *Bergaueria* in the Lower Cambrian Gog Group near Lake Louise, Alberta. *Journal of Paleontology* 64:436–440.

Porada H, Ghergut J, Bouougri EH. 2008. *Kinneyia*-type wrinkle structures—critical review and model of formation. *Palaios* 23:65–67.

Pratt BR. 1998a. Syneresis cracks: subaqueous shrinkage in argillaceous sediments caused by earthquake-induced dewatering. *Sedimentary Geology* 117:1–10.

Pratt BR. 1998b. Molar-tooth structure in Proterozoic carbonate rocks; origin from synsedimentary earthquakes, and implications for the nature and evolution of basins and marine sediment. *Geological Society of America Bulletin* 110:1028–1045.

Pratt BR. 2002. Storms versus tsunamis: dynamic interplay of sedimentary, diagenetic, and tectonic processes in the Cambrian of Montana. *Geology* 30:423–426.

Reineck H-E, Singh IB. 1980. *Depositional Sedimentary Environments*: Springer, Berlin. 549 p.

Retallack GJ. 1991. *Miocene Paleosols and Ape Habitats of Pakistan and Kenya*: Oxford University Press, New York. 346 p.

Retallack GJ. 1992. What to call early plant formations on land? *Palaios* 7:508–520.

Retallack GJ. 1994. A pedotype approach to latest Cretaceous and earliest Tertiary paleosols in eastern Montana. *Bulletin of the Geological Society of America* 106:1377–1397.

Retallack GJ. 2001. *Soils of the Past*: Blackwell, Oxford, UK. 404 p.

Retallack GJ. 2008. Cambrian paleosols and landscapes of South Australia. *Australian Journal of Earth Sciences* 55:1083–1106.

Retallack GJ. 2009a. Cambrian–Ordovician non-marine fossils from South Australia. *Alcheringa* 33:355–391.

Retallack GJ. 2009b. Early Paleozoic pedostratigraphy and global events in Australia. *Australian Journal of Earth Sciences* 56:569–584.

Retallack GJ. 2009c. Greenhouse crises of the past 300 million years. *Geological Society of America Bulletin* 121:1441–1455.

Retallack GJ. 2010. Lateritization and bauxitization events. *Economic Geology* 105:655–667.

Retallack GJ. 2011a. Neoproterozoic glacial loess and limits to snowball Earth. *Geological Society of London Journal* 168:1–19.

Retallack GJ. 2011b. Problematic megafossils in Cambrian palaeosols of South Australia. *Palaeontology* 54:1223–1242.

Retallack GJ. 2012a. Criteria for distinguishing microbial mats and earths. *In* Noffke N, Chafetz H (Editors). *Microbial Mats in Siliciclastic Sediments*, Special Publication 101: SEPM Society for Sedimentary Geology, Tulsa, Oklahoma. p. 136–152.

Retallack GJ. 2012b. Were Ediacaran siliciclastics of South Australia coastal or deep marine? *Sedimentology* 59:1208–1236.

Retallack GJ, Huang C-M. 2011. Ecology and evolution of Devonian trees in New York, USA. *Palaeogeography, Palaeoclimatology, Palaeoecology* 299:110–128.

Retallack GJ, Mindszenty A. 1994. Well preserved Late Precambrian paleosols from northwest Scotland. *Journal of Sedimentary Research* A64:264–281.

Retallack GJ, Roering JG. 2012. Wave-cut or water-table platforms of rocky coasts and rivers? *GSA Today* 22(6):4–9.

Retallack GJ, Sheldon ND, Cogoini M, Elmore RD. 2003. Magnetic susceptibility of Early Paleozoic and Precambrian paleosols. *Palaeogeography, Palaeoclimatology, Palaeoecology* 198:373–380.

Rose EC. 2006. Nonmarine aspects of the Cambrian Tonto Group of the Grand Canyon, USA, and broader implications. *Palaeoworld* 15:223–241.

Rye R, Holland HD. 1998. Paleosols and the evolution of atmospheric oxygen; a critical review. *American Journal of Science* 298:621–672.

Schlyter P. 2006. Ventifacts as palaeo-wind indicators in southern Scandinavia. *Permafrost and Periglacial Processes* 6:207–219.

Seilacher A. 2007. *Trace Fossil Analysis*: Springer, Berlin. 226 p.

Sheldon ND, Retallack GJ, Tanaka S. 2002. Geochemical climofunctions from North American soils and application to paleosols across the Eocene–Oligocene boundary in Oregon. *Journal of Geology* 110:687–696.

Sheldon ND, Tabor NJ. 2009. Quantitative paleoenvironmental and paleoclimatic reconstruction using paleosols. *Earth-Science Reviews* 95:1–52.

Soil Survey Staff. 2000. *Keys to Soil Taxonomy*: Pocahontas Press, Blacksburg, West Virginia. 600 p.

Southard JB, Lambie JM, Federico DC, Pile HT, Weidman CR. 1990. Experiments in bed configurations in fine sands under bidirectional purely oscillatory flow, and the origin of hummocky cross-stratification. *Journal of Sedimentary Petrology* 60:1–17.

Stone J, Lambeck K, Field LK, Evans JM, Creswell RG. 1996. A late glacial age for the Main Rock Platform, western Scotland. *Geology* 24:707–710.

Taylor G, Eggleton RA. 2001. *Regolith Geology and Geomorphology*: Wiley, Chichester, UK. 375 p.

Torell O. 1870. Petrifacta suecana formationis Cambricae. *Lunds Universitets Årsskrift* 6(8):1–14.

Vepraskas MJ, Sprecher SW. 1997. Summary. *In* Vepraskas MJ, Sprecher SW (Editors). *Aquic Conditions and Hydric Soils: The Problem Soils*, Special Publication 150: Soil Science Society of America, Madison, Wisconsin. p. 153–156.

Vintaned JAG, Liñan E, Mayoral E, Dies ME, Gonzalo R, Muñiz F. 2006. Trace and soft body fossils from the Pedroche Formation (Ovetian, Lower Cambrian of the Sierra de Cordoba, S. Spain) and their relation to the Pedroche event. *Geobios* 39:443–468.

Walcott CD. 1917. Cambrian geology and paleontology, IV, No. 2, The *Albertella* fauna in British Columbia and Montana. *Smithsonian Miscellaneous Collections* 67(2444):7–8.

Watanabe Y, Martini JEJ, Ohmoto H. 2000. Geochemical evidence for terrestrial ecosystems 2.6 billion years ago. *Nature* 408:574–578.

Webby BD. 1970. Late Precambrian trace fossils from New South Wales. *Lethaia* 3:79–109.

Weinberger R. 2001. Evolution of polygonal patterns in stratified mud during desiccation; the role of flow distribution and layer boundaries. *Geological Society of America Bulletin* 113:20–31.

Went DJ. 2005. Pre-vegetation alluvial fan facies and processes: an example from the Cambro–Ordovician Rozel Conglomerate Formation, Jersey, Channel Islands. *Sedimentology* 52:693–713.

Wilson CG, Matisoff G, Whiting PJ. 2007. The use of ^{7}Be and $^{210}Pb_{xs}$ to differentiate fine suspended sediment sources in South Slough, Oregon. *Estuaries and Coasts* 30:348–358.

Winston D, Lange I, Bleiwas D, Godlewski D. 1977. Alluvial fan, shallow water and sub-wavebase deposits of the Belt Supergroup near Missoula, Montana. *30th Annual Meeting Rocky Mountain Section Geological Society of America Field Trip Guide* 5:1–41.

Yochelson EL, Fedonkin MA. 1997. The type specimens (Middle Cambrian) of the trace fossil *Archaeonassa* Fenton and Fenton. *Canadian Journal of Earth Sciences* 34:1210–1219.

Young FG. 1972. Early Cambrian and other trace fossils from the southern Cordillera of Canada. *Canadian Journal of Earth Sciences* 9:1–17.